Lytic bacteriophages facilitate antibiotic sensitization of *Enterococcus faecium*

Gregory S. Canfield,[a,b] Anushila Chatterjee,[b] Mihnea R. Mangalea,[b] Emma K. Sheriff,[b] Micah Keidan,[b] Sara W. McBride,[b,*] Bruce D. McCollister,[a] and Breck A. Duerkop[b,#]

[a]Division of Infectious Diseases, University of Colorado School of Medicine, Aurora, Colorado, USA

[b]Department of Immunology and Microbiology, University of Colorado School of Medicine, Aurora, Colorado, USA

[#]Correspondence: Breck A. Duerkop breck.duerkop@cuanschutz.edu

[*]Current address: Salk Institute, La Jolla, California, USA

Running Title: Phages enhance antibiotic susceptibility of *E. faecium*

Key words: bacteriophages, *Enterococcus*, antibiotic resistance, phage–bacteria interactions, phage resistance, cephalosporin, beta-lactams

Abstract

Enterococcus faecium, a commensal of the human intestine, has emerged as a hospital-adapted, multi-drug resistant (MDR) pathogen. Bacteriophages (phages), natural predators of bacteria, have regained attention as therapeutics to stem the rise of MDR bacteria. Despite their potential to curtail MDR *E. faecium* infections, the molecular events governing *E. faecium*-phage interactions remain largely unknown. Such interactions are important to delineate because phage selective pressure imposed on *E. faecium* will undoubtedly result in phage resistance phenotypes that could threaten the efficacy of phage therapy. In an effort to understand the emergence of phage resistance in *E. faecium*, three newly isolated lytic phages were used to demonstrate that *E. faecium* phage resistance is conferred through an array of cell wall-associated molecules, including secreted antigen A (SagA), enterococcal polysaccharide antigen (Epa), wall teichoic acids, capsule, and an arginine-arginine-aspartate (RDD) protein of unknown function. We find that capsule and Epa are important for robust phage adsorption and that phage resistance mutations in *sagA*, *epaR*, and *epaX* enhance *E. faecium* susceptibility to ceftriaxone, an antibiotic normally ineffective due to its low affinity for enterococcal penicillin binding proteins. Consistent with these findings, we provide evidence that phages potently synergize with cell wall (ceftriaxone and ampicillin) and membrane-acting (daptomycin) antimicrobials to slow or completely inhibit the growth of *E. faecium*. Our work demonstrates that the evolution of phage resistance comes with fitness defects resulting in drug sensitization and that lytic phages could potentially serve as antimicrobial adjuvants in treating *E. faecium* infections.

Introduction.

Enterococci are intestinal commensal bacteria and important opportunistic human pathogens (1). Of the two most clinically relevant enterococcal species, *Enterococcus faecalis* and *Enterococcus faecium*, the emergence of multidrug resistance is observed most commonly with *E. faecium* (2). Considering that effective antibiotics with activity against multidrug-resistant (MDR) *E. faecium* are limited, clinicians are often forced to use antibiotic combination therapy to treat these infections (3). Although this approach can be life-saving, these regimens increase the risk of patient adverse drug events, drug-drug interactions, dysbiosis, and may fail to cure the infection (4). Rising from desperate treatment dilemmas like these are several examples of the successful use of phage therapy to treat MDR bacterial infections in humans (5-8). These success-stories have motivated renewed interest in the use of phage therapy for treatment of bacterial infections. Despite this motivation, relatively little is understood about the bacterial receptors exploited by phages to infect their bacterial hosts and the counter-measures employed by bacteria to avoid phage infection. We believe that understanding the molecular events that lead to phage resistance in MDR bacteria may help mitigate the threat of phage therapy failure.

Recently, our group and others have begun to elucidate the molecular mechanisms that enable successful phage infection of enterococci and the bulk of these studies were performed for *E. faecalis* and its interactions with tailed dsDNA phages. (9-15). The molecular mechanisms enabling phage infection in *E. faecium* are not well studied. Our knowledge of potential *E. faecium* phage receptors comes from an *in vitro* study where phage and *E. faecium* co-existence was challenged through multiple passages in laboratory media (12). Whole genome sequencing of phage resistant survivors showed mutations in the capsule tyrosine kinase *ywqD2* (equivalent to *wze*), RNA polymerase β-subunit (*rpoC*), several predicted hydrolases, and a cell wall precursor enzyme. It was proposed that these mutations conferred phage resistance, though direct genetic testing of this hypothesis was not performed. Tandem-duplications in a putative phage tail fiber gene (EFV12PHI1_98) supported evolution of phages that overcame adaptive changes that resulted in phage resistance of *E. faecium* (12).

In this work, we expand on our understanding of phage-enterococcal interactions by identifying genes important for lytic phage infection of *E. faecium.* We have isolated three previously uncharacterized *E. faecium*-specific phages and show that each belong to the *Siphoviridae* morphotype of the *Caudovirales* and resemble previously described lytic enterococcal phages (9-11, 14). Protein coding sequence comparison to other enterococcal phages reveals that one phage belongs to a novel enterococcal phage orthocluster and the remaining two phages belong to previously described enterococcal phage orthoclusters (16). To identify the molecular determinants of *E. faecium* phage infection, we used these three phages to generate a collection of *E. faecium* phage resistant mutants. Phage resistance mutations mapped to genes encoding the cell wall hydrolase secreted antigen A (*sagA*), putative teichoic acid precursors of the enterococcal polysaccharide antigen (*epa*), capsule biosynthesis enzymes, and an arginine-aspartate-aspartate (RDD) protein. Capsule and putative teichoic acid biosynthesis genes, but not SagA, were shown to mediate phage adsorption. Considering that all of the genes identified are involved in cell wall biochemistry and/or architecture, we determined if these phage resistance mutations result in fitness tradeoffs that lead to altered antimicrobial susceptibility. Phage resistant strains harboring mutations in *sagA*, *epaX*, and *epaR* showed enhanced susceptibility to cell wall and/or membrane-acting antibiotics, including ceftriaxone, ampicillin, and daptomycin. We discovered that combining phages with cell wall or membrane-acting antimicrobials acts synergistically to kill *E. faecium*. These findings suggest lytic phages might be leveraged as antibiotic adjuvants to offset the emergence of multi-drug resistant strains of *E. faecium* in hospitalized patients.

Results.

Genome sequence analysis and morphology of novel lytic *E. faecium* bacteriophages. *E. faecium* phages 9181, 9183 and 9184 were isolated from raw sewage by plaque assay using *E. faecium* clade B strains Com12 and 1,141,733 (17). Evaluation of phage morphology by TEM revealed that all three phages were non-contractile tailed phages characteristic of the *Siphoviridae* morphotype (Fig. 1) (18). DNA sequence analysis demonstrated that the phage 9181, 9183 and 9184 genomes are

71,854bp, 86,301bp, and 44,601bp in length, respectively (Fig. 1). The genomes of phages 9181 and 9183 were assembled into single contigs. The phage 9184 genome assembled into two contigs, with a 53-bp sequencing gap located near the 5' end of a predicted BppU-family phage baseplate upper protein. In total, 123, 128, and 73 open reading frames (ORFs) were identified for phages 9181, 9183 and 9184, respectively (Table S1). Genome modularity based on predicted gene function was observed for each phage genome, however, for phage 9181 the lysin and holin genes are located at the 5' and 3' termini of the genome (Fig. 1). Functional classifications, consisting of replication or biosynthesis, DNA packaging, phage particle morphogenesis, nucleic acid restriction and modification, host cell lysis, sensory function, sugar transferase and potential β-lactamase, could be predicted for approximately 30%, 47%, and 48% of the phage 9181, 9183, and 9184 ORFs, respectively (Table S1). The remaining genes were predicted to be hypothetical genes or genes containing domains of unknown function. The absence of genes encoding Cro repressor-family proteins, toxin-antitoxin genes, and putative integrase genes (except for phage 9183, discussed below) indicates that that phages 9181, 9183, and 9184 are obligately lytic.

Comparative genome analysis places phages 9181, 9183, and 9184 in distinct orthoclusters.

Comparative genome analysis of phages 9181, 9183 and 9184 was performed with all publicly available enterococcal phage genomes using OrthoMCL, an algorithm that identifies clusters of orthologous proteins from at least two phages enabling phylogenetic categorization of phage proteins into "orthoclusters" (16, 19). Of the 10 enterococcal phage orthoclusters originally identified by Bolocan et al. (16), OrthoMCL clustering places phage 9184 into orthocluster I and phage 9183 into orthocluster X (Fig. 2). Phage 9181 forms a new orthocluster that we have named orthocluster XI (Fig. 2). Whole genome alignments of phages 9183 and 9184 to their nearest orthocluster neighbors, VPE25 and VFW for 9183 and vB_EfaS-DELF1 and IME-EFm5 for 9184, revealed conserved protein sequence identity and similar genome organization (Fig. S1A and S1B). Conversely, phage 9181 shared little protein sequence identity and genome organization to its nearest neighbors, phage EFC-1 and phage FL4A, supporting its placement as the sole member of a new orthocluster (Fig. S1C). Higher protein sequence

identity and more similar genome organization was observed for phages belonging to the same orthocluster rather than phages belonging to different orthoclusters. Since the publication of Bolocan et al., an additional 45 phage genomes have been made publically available, resulting in the identification of a 12th orthocluster consisting of phages EFA-1 and EFA-2, two recently described phages of unknown morphology (Fig. 2). Consistent with prior observations of orthocluster I phages, a β-lactamase domain-containing protein (ORF35) was found in the genome of phage 9184 (Fig. 1 and Table S1). Similar to phages in orthocluster X, an integrase-family recombinase was found in the genome of phage 9183 (Table S1). However, prior evidence demonstrates that other members of this orthocluster are unable to lysogenize their *E. faecalis* host (11).

***E. faecium* phages have broad and narrow tropism for laboratory and clinical *E. faecium* isolates.** We next sought to determine the host range of each phage against strains of *E. faecium* and *E. faecalis*. To achieve this, a phage susceptibility assay was performed by spotting 10-fold serially-diluted enterococcal cultures on Todd-Hewitt broth (THB) agar embedded with phages 9181, 9183 or 9184. A panel of 10 laboratory *E. faecium* isolates and 11 contemporary MDR clinical *E. faecium* isolates were selected for this analysis (Table S4) (17). An *E. faecium* strain was considered phage-susceptible if less than 1 x 10^5 CFU/mL were recovered following phage exposure, representing greater than 4-log of bacterial killing. Phages 9181 and 9183 demonstrated narrow host ranges against laboratory *E. faecium* strains (Fig. 3A). Besides the host strain on which the phage was isolated (Com12 for phage 9181 and 1,141,733 for phage 9183), only *E. faecium* Com15 was susceptible to phage 9181, while no other *E. faecium* laboratory strain tested was susceptible to phage 9183. Contrarily, 60% of the laboratory *E. faecium* strains were susceptible to phage 9184 (Fig. 3A). There was an absence of susceptibility to phage 9181 and 9183, and reduced susceptibility (~36%) to phage 9184 for the contemporary MDR clinical *E. faecium* isolates (Fig. 3B). Together these data show that phage 9184 has a broader host range compared to phages 9181 and 9183. Interestingly, *E. faecium* 1,231,501 and 1,230,933, the latter of which is multi-drug resistant, lacked susceptibility to phage 9181, 9183 and 9184. None of the three phages were capable of infecting any of the 10 clinical *E. faecalis*

163 strains tested (designated UCH12-20 in Table S4), suggesting that these phages are specific for *E.*
164 *faecium*.
165
166 **Phage predation elicits spontaneous and stable phage resistance in *E. faecium*.** To identify *E.*
167 *faecium* genes that are involved in phage infection, we isolated spontaneous phage-resistant *E.*
168 *faecium* strains following exposure to phages 9181, 9183 and 9184. Phage-resistant isolates were
169 identified by plating stationary phase cultures of *E. faecium* Com12 and 1,141,733 on THB agar
170 embedded with phages 9181, 9183, or 9184. Colonies that arose on these plates represented potential
171 phage-resistant colonies. To confirm the stability of the phage-resistant phenotype, a colony was
172 serially passaged daily for 3 days on THB agar before re-streaking again on phage embedded THB
173 agar. The growth of a strain in the presence of phage following serial passage suggested a stable
174 phage-resistant phenotype (Fig. 4A-C). For phages 9181 and 9183 resistant *E. faecium* strains
175 (denoted 81R3-8 and 83R1-8, respectively) we observed bacterial growth in the presence of phages to
176 levels that were similar to bacterial growth in the absence of phages indicating a strong resistance
177 phenotype (Fig. 4A, 4B and Fig. S2A, S2B, S2D, S2E). However, for phage 9184 we observed limited
178 phage resistance in all but one presumed *E. faecium* phage resistant isolate (Fig. 4C and Fig. S2C,
179 S2F) suggesting that robust resistance to phage 9184 may be multifactorial.
180
181 ***E. faecium* phage resistance mutations occur in cell wall biosynthesis and architecture genes**
182 **and a gene encoding a transmembrane protein.** To identify genetic changes conferring a phage
183 resistance phenotype, we performed whole genome DNA sequencing of phage resistant and parental
184 *E. faecium* strains. We observed unique and conserved genome mutations in strains that had
185 developed phage resistance (Fig. 5A-D and Table S2).
186 Five of six mutations identified in phage 9181-resistant strains were detected in *efvg_rs16270*,
187 which in the *E. faecium* Com12 reference genome is annotated as a hypothetical protein and was
188 flanked by a 5' sequencing gap. Closure of this sequencing gap by PCR and amplicon sequencing
189 revealed that *efvg_rs16270* encodes the *E. faecium* secreted antigen A (SagA) protein. Whole genome

sequencing showed that all *sagA* mutations localized at or near the peptidoglycan clamp or active site residues of the NlpC_P60 hydrolase domain of SagA, which was recently shown to function as an endopeptidase that cleaves crosslinked Lys-type peptidoglycan fragments (Fig. 5A and Table S2A) (20). To determine the impact of *sagA* mutations on protein structure and function, each single nucleotide polymorphism-associated *sagA* mutant was assessed by Missense 3D analysis (21). BLASTp alignment of SagA from *E. faecium* Com12 and Com15 showed 95% identity along the entire length of the protein and *E. faecium* Com12 and Com15 exhibit identical protein homology in the NlpC_P60 hydrolase domain (Fig. S3), suggesting that SagA should be functionally conserved between these two stains. Therefore, we used the *E. faecium* Com15 NlpC_P60 crystal structure (PDB 6B8C) in Missense 3D to assess the impact of residue changes on the structure and function of NlpC_P60 hydrolase in our *sagA* mutant strains (20). Except for one SagA mutant (81R8; G435V), no structural damaging mutations were found. Given that the potential for structural damage in our *sagA* mutants was low, the observation that all mutations occurred in the NlpC_P60 hydrolase domain, and the fact that *sagA* has been shown to be an essential gene in *E. faecium*, we suspect that these *sagA* mutants represent hypomorphs whose expression levels or catalytic activity are reduced (20, 22, 23). Interestingly, hypomorphs have been observed in the *E. faecalis* SagA-like peptidoglycan hydrolase SalB (24). We complemented the *sagA* mutations in phage 9181 resistant strains using a construct previously generated, pAM401-*sagA*, which carries the *sagA* gene and its native promoter from *E. faecium* Com15 (22). For all *sagA* mutants, complementation with pAM401-*sagA* restored phage susceptibility (Fig. S4A). This results suggests that non-crosslinked peptidoglycan in *E. faecium* Com12 is essential for phage 9181 infection.

One phage 9181-resistant strain (81R7) harbored mutations in capsule tyrosine kinase (*wze*) and topoisomerase III (*topB*) genes and lacked a *sagA* mutation (Table S2A). Similarly, sequencing analysis of all 9184 resistant strains (84R1-6) revealed an assortment of mutations in the capsule biosynthesis locus. Nonsense, insertion and deletion mutations were detected in *wze*, capsule aminotransferase (*efsg_rs08090*), capsule polymerase (*wzy*), and capsule nucleotide sugar dehydrogenase (*efsg_rs08120*) genes (Fig. 5B and Table S2C). Prior co-evolution experiments

between the *Myoviridae* phage 1 and *E. faecium* TX1330 revealed a propensity for *wze* mutations within an evolved phage resistant *E. faecium* population (12). Our data is consistent with this observation and suggests that *E. faecium* capsule might serve as a possible receptor and/or adsorption factor for phages 9181 and 9184. Despite the abundance of capsule mutations detected among our mutant strains, complementation of capsule alleles in capsule mutants minimally restored or failed (Fig. S4B-C) to restore phage 9181 and 9184 susceptibility. This result suggests that capsule is not a major receptor mediating phage resistance to phage 9181 (Fig. S4B) and only weakly promotes phage 9184 resistance (Fig. S4C). These results emphasize the importance of other non-capsule associated mutations in conferring phage-resistance to phage 9181 (*sagA*) and phage 9184. We attempted to address the non-capsule associated mutation in strain 81R7 (*topB*) and its involvement in phage 9181 resistance, however, all attempts to clone *topB* into the expression vector pLZ12A resulted in truncated *topB* inserts following transformation into *Escherichia coli*, suggesting that constitutive expression of *E. faecium topB* may be toxic to *E. coli*. Similarly, to address the role of the non-capsule mutation detected in 84R6, which exhibited a robust phage 9184-resistance phenotype, a predicted arginine-aspartate-aspartate gene (*rdd*), this gene was successfully cloned into pLZ12A yet transformation of this construct into *E. faecium* 84R6 was unsuccessful despite repeated attempts. Given the ease with which pLZ12A-*wze* and empty pLZ12A vector were transformed into *E. faecium* 84R6 and our repeated failure to successfully recover transformants harboring pLZ12A-*rdd* suggests that over-expression of *rdd* in *E. faecium* 84R6 may be lethal.

Analysis of *E. faecium* phage 9183 resistant strains (83R1-8) identified mutations in *epa* genes, *epaR* and *epaX* (Fig. 5D and Table S2B). Mutation of *epaR* and *epaX* results in *E. faecalis* phage resistance (9, 10, 14) and recently it was determined that the *epaR* and *epaX* genes of *E. faecalis* V583 participate in wall teichoic acid biosynthesis (25). Considering that mutation of the *epaX* homologs *epaOX* and *epaOX2* from *E. faecalis* OG1RF conferred phage VPE25-resistance by limiting phage adsorption (10, 11), we suspect that teichoic acids also mediate adsorption of phage 9183 to *E. faecium* 1,141,733. We were surprised that we did not find any phage 9183 resistant strains with mutations in PIP_{EF}, given the high protein homology and similar genome organization observed

between phages 9183, VPE25 and VFW, the latter two which use PIP_{EF} as a receptor (11) (Fig. 2). To confirm that mutations in the *epa* locus confer phage resistance in *E. faecium*, we pursued a similar complementation strategy as above with the *epaR* and *epaX* mutants identified in the phage 9183-resistant mutants. All phage 9183-resistant mutants complemented with either the *epaR* or *epaX* were restored for phage susceptibility (Fig. S4D). Given the importance of D-alanylation in teichoic acid biosynthesis, we performed complementation with pLZ12A-*dltA* in the *epaX* and *dltA* double mutant (83R7). We observed that only pLZ12A-*epaX*, not pLZ12A-*dltA*, was capable of restoring phage susceptibility in 83R7 (Fig. S4D). Considering that EpaX acts upstream of DltA in the biosynthesis of teichoic acids (25), these data suggest that *dltA* is dispensable during phage infection, lending further support to the notion that the *epa* variable locus involved in teichoic acid biosynthesis is a driver of *E. faecium* infection by phage 9183.

***E. faecium* phage resistant mutants have phage adsorption defects.** To determine if phage adsorption defects occur due to phage resistance, we sought to quantify phage 9181, 9183, and 9184 adsorption to wild type and phage resistant *E.* faecium strains using a phage attachment assay (9, 10, 14). For phage 9181 resistant strains, we observed no significant change in adsorption to *sagA* mutant strain 81R5 and a modest change in phage adsorption to the phage resistant strain 81R7 harboring a *wze* and *topB* mutations (Fig. 6A). This result suggests that mutation of *sagA* in *E. faecium* Com12 has little to no effect on phage 9181 adsorption. It is possible that mutation of *wze* contributes to phage binding, however, we cannot rule out the possibility that mutation of *topB* in this mutant background causes transcriptional or translational changes in surface expressed molecules that result in the modest phage 9181 adsorption phenotype (Fig. 6A).

Previous work has demonstrated that *epa* mutants exhibit phage adsorption defects in *E. faecalis* (9, 10, 13, 14). Since we observed *epa* mutations that conferred phage 9183 resistance, we sought to determine if *epa* mutations might promote a similar phenotype in *E. faecium*. We observed a reduction in phage 9183 adsorption to mutants possessing *epaR* (83R6 and 83R8) and *epaX* (83R4 and 83R7) mutations compared with the parental strain (Fig. 6B). Although *epaX* mutants 83R4 and

83R7 were noted to also have mutations in *gdh* and *dltA*, respectively, we suspect that EpaX was the driver of this phenotype because of the known role of *epaX* homolog mutations to inhibit phage VPE25 adsorption to *E. faecalis* and that EpaX functions upstream of DltA in the biosynthesis of teichoic acid (10, 25). Taken together, these results suggest that mutations in the *epa* locus of *E. faecium* lessen phage 9183 adsorption to the surface of its host strain.

To determine if mutations in the capsule locus facilitated phage 9184 adsorption defects, we performed phage 9184 adsorption assays using wild type and phage 9184 resistant mutants. We observed significant deficits in phage adsorption to strains harboring mutations in capsule polymerase (84R1), nucleotide sugar dehydrogenase (84R4), and tyrosine kinase (84R6) in comparison to the parental strain (Fig. 6C). Given that 84R6 also harbors an *rdd* mutation which encodes a putative transmembrane protein, we cannot definitively conclude that the adsorption deficit was related to the capsule tyrosine mutation, as this mutation only manifested as a mild adsorption defect for phage 9181 (Fig. 6A). Considering the adsorption defect is greater for the capsule mutants raised against phages 9184 compared to the phage 9181 capsule mutant 81R7, it is possible that additional surface associated molecules mediate the attachment of phage 9181 to *E. faecium* cells. Together, these data indicate that *E. faecium* capsule contributes to phage adsorption and may be phage specific.

***E. faecium* phage resistance enhances β-lactam and lipopeptide susceptibility.** With renewed interest focused on utilizing lytic phages for the treatment of bacterial infections and the observation that phage resistance can be a fitness tradeoff under antibiotic pressure (26, 27), we sought to determine the impact of *E. faecium* phage resistance on antimicrobial susceptibility. We performed antimicrobial susceptibility screening using E-test strips for the phage 9181, 9183, and 9184 resistant mutants compared to their parental strains to determine if phage resistance altered *E. faecium* antimicrobial susceptibility. For phage 9181 resistant mutants, we observed a 2-5 fold reduction in the minimum inhibitory concentration (MIC) of ampicillin and an 8-32 fold reduction in the MIC of ceftriaxone (Table S3A). Interestingly, the enhancement of ampicillin and ceftriaxone susceptibility correlated with phage 9181 resistant mutants harboring mutations in *sagA*, and not *wze* or *topB*. For

phage 9183 resistant mutants, we also observed a 5-8 fold reduction in the MIC of ampicillin and 16-128 fold reduction in the MIC of ceftriaxone (Table S3B). Additionally, we noted a 1.5-3 fold reduction in the MIC of daptomycin, a lipopeptide class antimicrobial, which was not observed for the phage 9181 resistant mutants. These results suggest that the acquisition of phage resistance via mutation of *sagA* and *epa* genes in *E. faecium* is a fitness defect that manifests as enhanced β-lactam susceptibility.

No phage capsule mutants showed a significant difference in antimicrobial susceptibility to β-lactams or lipopeptides, suggesting that mutations to the *E. faecium* capsule locus and *rdd* avoid the cost of increased antimicrobial susceptibility (Table S3C).

Lytic phages synergize with β-lactam and lipopeptide antimicrobials to enhance the killing of *E. faecium*. Considering the antibiotic fitness cost associated with phage resistance in *E. faecium*, we hypothesized that phages 9181 and 9183 would be capable of synergizing with ampicillin, ceftriaxone, and daptomycin to kill *E. faecium*. To address this question, we performed phage-antibiotic synergy assays where *E. faecium* was grown in the presence of phages alone, sub-inhibitory concentrations of ampicillin, ceftriaxone, or daptomycin alone, or a combination of phage and a sub-inhibitory concentration of antibiotics (Fig. 7A-E). For all three antibiotics, we observed that the combination of phage and sub-inhibitory concentrations of antibiotics were able to inhibit the growth of *E. faecium* better than phage or antibiotic alone. Given the absence of growth inhibition of *E. faecium* in the presence of sub-inhibitory concentrations of antibiotics alone, this result is consistent with a synergistic antimicrobial interaction between phages and antibiotics. Interestingly, the synergy observed between phages 9181 and 9183 and ceftriaxone appeared more potent than the synergy observed between these phages and ampicillin (Fig. 7A-D). A dose-response relationship emerged when ampicillin was combined phages 9181 and 9183 where decreasing concentrations of ampicillin enabled varying degrees of bacterial population recovery (Fig. 7A-B). These data suggest that phages 9181 and 9183 could serve as useful adjuvants in combination with β-lactams for the treatment of *E. faecium* infections by restoring the susceptibility to *E. faecium* strains harboring intrinsic β-lactam resistance. We also observed that the combination of phage 9183 and daptomycin slowed the growth of *E. faecium*

1,141,733 more than phage 9183 alone or daptomycin alone (Fig. 7E). This suggests that phage 9183 also synergizes with daptomycin to inhibit *E. faecium* 1,141,733. These results are consistent with those observed by Morrisette et al. who observed synergy between the *Myoviridae* phage 113 and β-lactam (ampicillin, ertapenem and ceftaroline) and lipopeptide antimicrobials against daptomycin-resistant and tolerant strains of *E. faecium* (28).

Discussion.

Considering the treatment pitfalls due to worsening drug resistance in *E. faecium* and other bacterial pathogens, the biomedical community is revisiting the use of phage therapy. Since phage therapy's departure from 20th century Western Medicine, new technologies have emerged that have facilitated fine-scale resolution of phage-bacterial molecular interactions. Despite these advancements, for many bacteria, including *E. faecium*, the molecular factors exploited by phages for infection remain largely understudied (12). We believe that studying the molecular interactions of phages with their *E. faecium* hosts will inform rational approaches for future phage therapies against this pathogen.

In this work, we describe three novel lytic phages of *E. faecium*. Using protein coding orthology, we show that one of these phages, phage 9181, forms a new orthocluster from the ten previously described enterococcal phage orthoclusters (16). We show that these phages are specific for *E. faecium* and exhibit broad and narrow strain tropism. Using whole genome sequencing and comparative genomics, we provide evidence that *sagA*, *epa*, and capsule biosynthesis genes are important for phage infection of *E. faecium*. We were unable to fully assess if the genes *topB* and *rdd* are important in mediating phage 9181 and phage 9184 resistance, respectively. We suspect that these genes aid in phage-*E.faecium* interactions. Consistent with previous observations in *E. faecalis* (9, 10, 13, 14), we show that mutations in *epaR* and *epaX* limit phage 9183 adsorption to *E. faecium*. Similarly, we show for the first time that mutations in the capsule locus, which is absent in *E. faecalis* (17), limits phage 9181 and 9184 adsorption to *E. faecium*.

Our investigation into fitness tradeoffs associated with *E. faecium* phage resistance revealed enhanced susceptibility to cell wall and membrane-acting antibiotics. We demonstrated that phages

352 9181 and 9183 synergize with cell wall and membrane-targeting antibiotics to more potently inhibit *E.*
353 *faecium*. Importantly, this analysis revealed that phages 9181 and 9183 could sensitize *E. faecium* to
354 ceftriaxone, an antibiotic that normally promotes enterococcal colonization of the intestine due to
355 intrinsic resistance (29). Phage synergy with ceftriaxone is an important discovery as it suggests a
356 strategy to re-sensitize enterococci to a third-generation cephalosporin. Exposure to cell wall-acting
357 agents is recognized as a key event prior to hospital-acquired enterococcal infection in susceptible
358 patients and cephalosporin re-sensitization could have a broad impact on anti-enterococcal therapy (2,
359 30). Cephalosporin activity pressures the native intestinal microbiota altering its ecology and related
360 mucosal immunity, creating a scenario for enterococci to thrive and become dominant members of the
361 microbiota (30-33). In patients with weakened immune systems or made vulnerable from hospital
362 procedures such as surgeries, bone marrow ablative chemotherapy, or pre-existing alcoholic
363 hepatitis/cirrhosis, these ceftriaxone-associated conditions can tip the scale in favor of infection (30-32,
364 34, 35). Even in *E. faecium* strains with ampicillin susceptibility, synergy with ceftriaxone for the
365 treatment of endocarditis was demonstrated to be not absolute, suggesting that current Infectious
366 Disease Society of America guidelines for the treatment of *E. faecium* endocarditis may lead to sub-
367 optimal results (36, 37). Combination therapy with phage and cell wall or membrane-acting
368 antimicrobials may offer a potential solution to circumvent this issue, while avoiding the risk associated
369 with exposing patients to combination β-lactam agents.

370 Previous studies indicate that intrinsic resistance to ceftriaxone is derived from not only a low-
371 affinity penicillin binding protein 5 (Pbp5), but also *pbpA*, *ponA* and *pbpf* genes in *E. faecium* (38-41).
372 However, in *ponA* and *pbpf* mutants a dissociation in penicillin and cephalosporin susceptibility was
373 observed in *E. faecium* whereby these mutants were rendered susceptible to cephalosporins, but unlike
374 a *pbp5* mutant, not ampicillin, (40). Interestingly, PbpA was found to be essential in *E. faecium* and also
375 exhibited low affinity for both ampicillin and ceftriaxone (38). Combining this observation with the
376 enhancement of ampicillin and ceftriaxone susceptibility displayed by *sagA*, *epaR* and *epaX* mutants, it
377 suggests that Pbp5 and PbpA may play a role in conferring β-lactam susceptibility in these phage
378 resistant mutants. However, to further add to the complexity of enterococcal cell wall dynamics, L,D-

transpeptidases (LDTs), a novel class of enzymes that function apart from Pbps to promote penicillin and cephalosporin, but not carbapenem resistance, may also contribute to this phenotype (42, 43). It is possible that mutations in *sagA*, *epaR*, and/or *epaX* alter expression levels or post-translational modification of Pbps or LDTs against ceftriaxone and ampicillin. An alternative hypothesis is that *sagA*, *epaR*, and *epaX* gene mutations may manifest their effects through interaction with peptidoglycan and the mechanism of enhanced β-lactam susceptibility may be exclusive from the activity of Pbps or LDTs. Consistent with this notion, mutation of a secreted peptidoglycan hydrolase in *E. faecalis*, *salB*, demonstrated enhanced susceptibility to cephalosporins. Pairwise amino acid alignment of *E. faecium* Com12 SagA and *E. faecalis* SalB revealed 51% identity over the N-terminal coiled-coil domain region, which is expected given their different C-terminal hydrolase domains (SCP in SalB; NlpC_P60 in SagA). Contrary to *sagA* in *E. faecium*, *salB* was shown to be non-essential in *E. faecalis*, and has a homolog (*salA*) which may partly compensate for the function of *salB* to maintain cell viability (24). Staining of an *E. faecalis salB* mutant with a non-specific, fluorescent Pbp antibody (Bocillin FL) revealed no difference from wild type. However, this analysis was performed in the absence of ceftriaxone pre-treatment, potentially masking subtle changes in the abundance of Pbps in the *salB* mutant at the cell wall (38). Therefore, it remains unclear if *salB* partners with or coordinates the activity of Pbps or LDTs to induce cephalosporin resistance. A *sagA* mutant described in our study (81R5; G460A) has a mutation residing two residues upstream from a peptidoglycan clamp residue (W462) and lacked enhanced susceptibility to ampicillin and ceftriaxone. The reason for this exception and why this mutation confers phage resistance is unclear.

The enhanced susceptibility to β-lactams in *epaR* and *epaX* in *E. faecium* mutants was surprising given prior reports of increased β-lactam resistance in *epa* mutants in *E. faecalis* (44). However, we note that all *epa* mutants tested in that analysis harbored mutations in genes from the core region of *epa* locus (i.e. *epaA*, *epaE*, *epaL*, *epaN*, *epaB*). To the best of our knowledge, this is the first report demonstrating enhanced β-lactam sensitivity to *epa* variable region mutants in enterococci. We observed enhanced susceptibility to daptomycin in *E. faecium epaR* and *epaX* mutants, consistent with data from *E. faecalis epaR* and *epaX* mutants (9, 14, 45). Given that the *epa* variable genes have

recently been discovered to be involved in teichoic acid biosynthesis (25), we hypothesize that altered display of teichoic acids at the cell surface enables the differential β-lactam and daptomycin susceptibility observed in *epa* core versus variable region mutants in enterococci. This hypothesis is supported by observations in *Staphylococcus aureus*, where metabolic perturbations leading to enhanced teichoic acid output or teichoic acid D-alanylation correlate with daptomycin tolerance (46-48). Similarly, mutation of *lafB*, a gene encoding lipoteichoic acid glycosyltransferase, induces a daptomycin hypersusceptible phenotype in *E. faecium* (49). Mutation of *bgsB* in *E. faecalis*, which functions with a *lafB* homolog (*bgsA*) in lipoteichoic acid anchor biosynthesis, results in enhanced susceptibility to daptomycin (14). A reduction in susceptibility to the β-lactam piperacillin in *lafB* (*E. faecium*) or *bgsB* (*E. faecalis*) mutants is reminiscent of the effect of *epa* core region mutations in enterococci (44). A similar pattern of enhanced daptomycin susceptibility at the cost of reduced β-lactam susceptibility, known as the see-saw effect (50), suggests that the altered display or abundance of the wall teichoic acids at the cell surface may occur in response to the modification of rhamnopolysaccharide or lipoteichoic acid. Mutation of *epaR* or *epaX* in *E. faecium* would potentially avoid the daptomycin-β-lactam see-saw effect, making phages that induce these mutations in enterococci attractive antimicrobial candidates. Collectively, these observations suggest that the location of *epa* mutations, core versus variable region, as well mutations in genes participating in lipoteichoic acid biosynthesis, are likely to impact the trajectory of β-lactam and daptomycin susceptibility in enterococci.

E. faecalis epa mutations are detrimental during intestinal colonization and show reduced virulence in a mouse peritonitis infection model (9, 51, 52). *epa* mutants are more susceptible to bile salts, neutrophils, exhibit reduced biofilm formation, and are unable to invade biotic and abiotic surfaces (45, 52-54). Therefore, we predict that *epaR* and *epaX* mutants in *E. faecium* will show a similar intestinal colonization dysfunction. Hydrolase-domain mutations in SagA are also likely to induce fitness costs *in vivo*. SagA was shown to promote *E. faecium* attachment to multiple connective tissue molecules, including fibrinogen, fibronectin, and collagen (23). Interestingly, peptidoglycan fragments released following SagA hydrolytic activity activates NOD2-mediated mucosal immunity in the intestine,

433 providing protection from *Salmonella enterica* infection and *Clostridioides difficile* colitis (20, 22). In *E.*
434 *faecalis,* mutation of the *sagA*-like gene *salB* altered cell morphology, increased biofilm formation,
435 impacted autolysis, and increased susceptibility to bile salts, detergent, ethanol, peroxide, and heat (55-
436 58). Contrary to SagA, cells expressing SalB were limited in binding fibronectin and collagen type I,
437 suggesting that these proteins exhibit different adherence capacities to host tissue. Considering these
438 observations together, it is possible that phage predation that promotes the formation of *sagA* mutants
439 would result in *E. faecium* cells that are compromised for adherence and/or invasion of host tissues,
440 and potentially less immunostimulatory during infection.

441 In conclusion, we have identified three previously undescribed phages that infect *E. faecium.*
442 The study of *E. faecium* resistance to these phages identified multiple components of the *E. faecium*
443 cell surface to be critical for productive phage infection. The enhanced sensitivity of *sagA*, *epaR* and
444 *epaX* mutants to cell wall and membrane acting antimicrobials suggests that these proteins represent
445 intriguing antimicrobial targets to be considered for future drug discovery efforts against *E. faecium*, and
446 potentially other Gram-positive pathogens harboring homologs of these genes. The finding that *E.*
447 *faecium* phages synergize with β-lactam and lipopeptide antibiotics provides encouragement that
448 phages could be used in combination with these antibiotics to increase their efficacy and possibly
449 repurpose such antibiotics that are currently deemed ineffective against enterococci.
450
451 **Materials and Methods.**
452 **Bacteria and bacteriophages.** A complete list of the bacterial strains and bacteriophages used in this
453 study can be found in Table S4. *E. faecium* Com12 was cultured in Todd-Hewitt broth (THB) and *E.*
454 *faecium* 1,141,733 was cultured in brain heart infusion (BHI) broth at 37ºC with rotation at 250 rpm. *E.*
455 *coli* strains were cultured in Lennox L broth (LB) at 37ºC with rotation at 250 rpm. Semi-solid media in
456 petri plates were made by adding 1.5% agar to broth prior to autoclaving. For antibiotic susceptibility
457 testing, Mueller Hinton Broth (MHB) was used. When needed, chloramphenicol was added to media at
458 20 µg/ml or 10 µg/ml for selection of *E. coli* or *E. faecium*, respectively. Phage susceptibility assays
459 were performed on THB agar supplemented with 10mM $MgSO_4$.

Bacteriophage isolation and purification. Phages 9181, 9183, and 9184 were isolated from wastewater obtained from a water treatment facility located near Denver, Colorado. Fifty milliliters of raw sewage was centrifuged at 3220 x *g* for 10 minutes at room temperature to remove debris. The supernatant was decanted and passed through a 0.45 µm filter. A 100µl aliquot of filtered wastewater was mixed with 130 µl of *E. faecium* 1,141,733 or Com12 diluted 1:10 from an overnight culture and incubated at room temperature for 15 min. Molten THB top agar (0.35%), supplemented with 10mM $MgSO_4$, was added to the bacteria-wastewater suspension and poured over a 1.5% THB agar plate supplemented with 10mM $MgSO_4$. Following overnight growth at 37ºC, plaques were picked with a sterile Pasteur pipette and phages were eluted from the plaque in 500 µl SM-plus buffer (100 mM NaCl, 50 mM Tris-HCl, 8 mM $MgSO_4$, 5 mM $CaCl_2$ [pH 7.4]) overnight (O/N) at 4ºC. After O/N elution, the phages were filter sterilized (0.45 µm). This procedure was repeated two more times to ensure clonal phage isolates. To amplify phages to high titer stocks, 10-fold serially diluted clonal phage isolates were mixed with their appropriate host strain diluted 1:10 from an O/N culture, incubated at room temperature and then poured over 1.5% THB agar supplemented with 10mM $MgSO_4$. Top agar from multiple near confluent lysed bacterial lawns were scraped into a 15 ml conical tube and centrifuged at 18000 x *g* for 10 minutes prior to decanting and 0.45 µm filter sterilization. Using these recovered phages, high-titer phage stocks were generated by infecting 500mL of early logarithmically (2-3 x 10^8 CFU/mL) growing *E. faecium* with phage at a multiplicity of infection of 0.5 following supplementation of media with 10mM $MgSO_4$. The phage-cell suspension was incubated at room temperature for 15 min and then incubated at 37ºC with rotation (200 rpm) for 4-6 hours. The cultures were centrifuged at 3220 x *g* for 10 minutes at 4ºC and the supernatants filtered (0.45µm). Clarified and filtered lysates were treated with 5 µg/ml each of DNase and RNase at room temperature for 1 hour and phages were precipitated with 1M NaCl and 10% (wt/vol) polyethylene glycol 8000 (PEG 8000) on ice at 4ºC overnight. Phage precipitates were pelleted by centrifugation at 11,270 x *g* for 20 minutes and resuspended in 2mL of SM-plus buffer. One-third volume chloroform was mixed by inversion into the phage precipitates and centrifuged at 16,300 x *g* to separate out residual PEG 8000 into the organic

phase. Phages in the aqueous phase were further purified using a cesium chloride gradient as described previously (11). The final titer was confirmed by plaque assay. Crude phage lysates were used for all phage susceptibility and adsorption assays, while cesium chloride gradient purified phages were used for phage genomic DNA isolation and transmission electron microscopy.

Transmission electron microscopy. 8 µl of 1 x 10^{10} pfu/ml of phages was applied to a copper mesh grid coated with formvar and carbon (Electron Microscopy Sciences) for 2 minutes and then gently blotted off with a piece of Whatman filter paper. The grids were rinsed by transferring between two drops of MilliQ water, blotting with Whatman filter paper between each transfer. Finally, the grids were stained using two drops of a 0.75% uranyl formate solution (a quick rinse with MilliQ water following the first drop followed by an additional 20 seconds of staining). After rinsing and blotting, the grids were allowed to dry for at least 10 minutes. Samples were imaged on a FEI Tecnai G2 Biotwin TEM at 80kV with an AMT side-mount digital camera.

Whole-genome sequence analysis of phages and phage-resistant bacteria. Phage DNA was isolated by incubating phages with 50 µg/ml proteinase K and 0.5% sodium dodecyl sulfate at 56ºC for 1 hour followed by extraction with an equal volume of phenol/chloroform. The aqueous phase was extracted a second time with an equal volume of chloroform and the DNA was precipitated using isopropanol. Bacterial DNA was isolated using a ZymoBIOMICS DNA miniprep kit (Zymo Research), following the manufacturers protocol. Phage and bacterial DNA samples were sequenced at the Microbial Genome Sequencing Center, University of Pittsburgh, using an Illumina NextSeq 550 platform and paired end chemistry (2 x 150bp). Paired-end reads were trimmed and assembled into contigs using CLC genomics workbench (Qiagen). Open reading frames (ORFs) were detected and annotated using rapid annotation subsystem technology (RAST) and the Phage Galaxy structural annotation (version 2020.1) and functional workflows (version 2020.3) (59, 60). Trimmed bacterial genomic reads for *E.* faecium Com12, 1,141,733, and phage resistant derivatives were mapped to reference genomes (GCF_000157635.1 (Com12); GCA_000157575.1 (1,141,733)), downloaded from the National Center

514 for Biotechnology Information (NCBI) website. To identify mutations conferring phage resistance the
515 basic variant detection tool from CLC genomics workbench was used to identify polymorphisms
516 (similarity fraction = 0.5 and length fraction =0.8).
517
518 **Enterococcal phage orthology analysis.** Enterococcal phage orthology was performed according to
519 a method described by Bolocan et al. (16). Briefly, publicly available enterococcal genomes were
520 downloaded from the Millard Lab phage genome database (http://millardlab.org/bioinformatics/). As of
521 May 15, 2020, there were 99 complete enterococcal phage genomes. Open reading frames for each
522 enterococcal phage genome were called using Prodigal and bacteriophage protein Orthologous Groups
523 were identified by OrthoMCL (19, 61). The resulting OrthoMCL matrix was used to generate an
524 orthology tree using the ggplot2 and ggdendro packages in R. Nearest neighbor phages to phages
525 9181, 9183, and 9184 from the OrthoMCL analysis were compared using the genome alignment
526 feature of ViP Tree using normalized tBLASTx scores between viral genomes to calculate genomic
527 distance for phylogenetic proteomic tree analysis (62).
528
529 **Routine molecular techniques, DNA sequencing, and complementation.** Confirmation PCRs were
530 performed using GoTaq Green master mix (Promega), per the manufacturer's instructions. Q5 DNA
531 polymerase master mix (New England Biolabs) was used for PCR reactions intended for cloning, per
532 the manufacturer's instructions. Plasmid DNA was purified using a QIAprep Miniprep kit (Qiagen) or a
533 ZymoPURE II Plasmid Midiprep kit (Zymo Research). Restriction enzymes and T4 ligase were
534 purchased from New England Biolabs. Sanger DNA sequencing was performed by Quintara
535 Biosciences (San Francisco, CA). A complete list of primers can be found in Table S4.
536 Complementation was performed using plasmid pLZ12A, a derivative of pLZ12 (63) carrying the *bacA*
537 promoter upstream of the multiple cloning site (9). *wze*, *epaX*, *dltA*, and *efsg_rs08090* were cloned into
538 pLZ12A as BamHI and EcoRI fragments. *epaR* and *efsg_rs08120* were cloned into pLZ12A as BamHI
539 and PstI fragments. Plasmids were transformed into *E. faecium* using a previously described glycine-
540 sucrose method (64, 65). Briefly, 1ml of overnight culture was inoculated into 50ml of BHI

supplemented with 2% glycine and 0.5M sucrose and grown overnight at 37°C with rotation (250 rpm). The following day the cells were pelleted at 7200 x *g* and re-suspended in an equal volume of pre-warmed BHI supplemented with 2% glycine and 0.5M sucrose and incubated for 1h at 37°C statically. The cells were pelleted at 7200 x *g* and washed three times in ice cold electroporation buffer (0.5M sucrose and 10% glycerol). 1-2 µg of plasmid DNA was electroporated into *E. faecium* using a Gene Pulser (Bio-Rad) with a 0.2 mm cuvette at 1.7kV, 200 Ω and 25 µF.

Phage susceptibility assay. Overnight bacterial cultures were pelleted, resuspended in SM-plus buffer, and normalized to OD_{600} of 1.0. 10-fold serial dilutions of bacteria were spotted on THB agar embedded with phage or THB agar alone, supplemented with 10mM $MgSO_4$. Phages were embedded at the following concentrations within THB agar: phage 9181 (10^8 PFU/ml), phage 9183 (10^7 PFU/ml), and phage 9184 (10^7 PFU/ml). Plates were incubated overnight at 37°C and viable CFU was determined by colony counting.

Isolation of phage-resistant *E. faecium* strains. 130 µl of a 1:10 dilution of *E. faecium* grown O/N was mixed with 10 µl of 10-fold serially diluted phages and added to 5 ml of prewarmed THB top agar (0.35% wt/vol). Phage-bacterium mixtures were poured onto the surface of THB agar plates (1.5% wt/vol). The plates were incubated at 37°C until phage-resistant colonies appeared in the zones of clearing. The presumptive resistant colonies were passaged four times by streaking single colonies onto THB agar.

Determination of phage host range. The host range of phages 9181, 9183, and 9184 were determined using a panel of laboratory and contemporary clinical *E. faecium* and *E. faecalis* isolates (Table S4). Overnight bacterial cultures were suspended in SM-plus buffer to an OD_{600} of 1.0 and 10-fold serially diluted and spotted on to THB agar containing phages. Plates were incubated O/N at 37°C and viable CFU was determined. Strains that exhibited greater than 4-log killing in the presence of

phage were termed phage susceptible, while those that grew beyond this threshold were considered phage resistant.

Phage adsorption assay. This assay was performed as described previously (10, 11). O/N bacterial cultures were pelleted at 3220 × *g* for 10 min and resuspended to 10^8 CFU/ml in SM-plus buffer. Phage adsorption was determined by mixing 5 x 10^6 pfu of phage and to 5 x 10^7 cfu of the appropriate bacterial strain in 500 µl and incubating statically at room temperature for 10 min. The bacteria-phage suspensions were centrifuged at 24,000 × *g* for 1 min, the supernatant was collected, and remaining phages enumerated by a plaque assay. SM-plus buffer with phage only (no bacteria) served as a control. Percent adsorption was determined as follows: $[(PFU_{control} - PFU_{test\ supernatant})/PFU_{control}] \times 100$. The fold change was calculated by dividing the percent adsorption of phage resistant mutants by those of parental strain.

Antibiotic MIC assay. Antibiotic MIC was determined for each strain using Etest strips (bioMérieux). Single colonies were grown O/N in 3mL of MHB broth at 37ºC with rotation (250 rpm). The following day overnight cultures were diluted to McFarland 0.5 in MHB broth and 100µL of the cell suspension was spread over the surface of MHB agar plates. One Etest strip was placed on the surface of the agar using sterile forceps. The plates were incubated for 18 hours at 37ºC. The MIC was determined to be the number closest to the zone of inhibition. The MIC reported for each strain is representative of two independent experiments.

Phage-antibiotic synergy assay. O/N cultures of *E. faecium* Com12 and *E. faecium* 1,141,733 were normalized to 10^8 CFU/mL. 100µl (10^7 CFU/mL) of bacteria was added into a sterile 96-well plate (Falcon) in triplicate. Antibiotics were diluted 1:100 into desired wells to achieve the appropriate final concentration. Phages were added to desired wells at 10^6 PFU/ml, achieving a multiplicity of infection of 0.1. The 96 well plate was loaded on to BioTek Synergy Plate reader pre-warmed to 37ºC, and agitated continuously for 18h, allowing for OD_{600} reading every 30 minutes.

Data availability. The Illumina reads for phage 9181, 9183, and 9184 and phage-resistant *E. faecium* mutants have been deposited in the European Nucleotide Archive under the accession number PRJEB39873. Assembled phage genomes were submitted to Genbank and were assigned the following accession numbers: MT939240 (phage 9181), MT939241 (phage 9183), and MT939242 (phage 9184).

Acknowledgements.

This work was supported by National Institutes of Health grants R01AI141479 (B.A.D.). We thank Dr. Jennifer Bourne at the University of Colorado School of Medicine Electron Microscopy Center for preparing and visualizing electron micrographs of phages. We thank the staff at the Microbial Genome Sequencing Center (MiGS) at the University of Pittsburgh for assistance with bacterial and phage whole genome DNA sequencing. We thank Dr. Howard Hang and Juliel Espinosa for generously providing pAM401-*sagA*.

References.

1. Arias CA, Murray BE. 2012. The rise of the Enterococcus: beyond vancomycin resistance. Nat Rev Microbiol 10:266-78.
2. Kristich CJ, Rice LB, Arias CA. 2014. Enterococcal infection—treatment and antibiotic resistance, p 1-62. *In* Gilmore MS, Clewell DB, Ike Y, Shakar N (ed), Enterococci : from commensals to leading causes of drug resistant infection [Internet]. Massachusetts Eye and Ear Infirmary, Boston, MA.
3. Beganovic M, Luther MK, Rice LB, Arias CA, Rybak MJ, LaPlante KL. 2018. A review of combination antimicrobial therapy for *Enterococcus faecalis* bloodstream infections and infective endocarditis. Clin Infect Dis 67:303-309.
4. Rybak MJ, McGrath BJ. 1996. Combination antimicrobial therapy for bacterial infections. Guidelines for the clinician. Drugs 52:390-405.
5. Fish R, Kutter E, Bryan D, Wheat G, Kuhl S. 2018. Resolving digital staphylococcal osteomyelitis using bacteriophage-a case report. Antibiotics (Basel) 7.
6. Cano EJ, Caflisch KM, Bollyky PL, Van Belleghem JD, Patel R, Fackler J, Brownstein MJ, Horne B, Biswas B, Henry M, Malagon F, Lewallen DG, Suh GA. 2020. Phage therapy for limb-threatening prosthetic knee *Klebsiella pneumoniae* infection: case report and in vitro characterization of anti-biofilm activity. Clin Infect Dis doi:10.1093/cid/ciaa705.

7. Schooley RT, Biswas B, Gill JJ, Hernandez-Morales A, Lancaster J, Lessor L, Barr JJ, Reed SL, Rohwer F, Benler S, Segall AM, Taplitz R, Smith DM, Kerr K, Kumaraswamy M, Nizet V, Lin L, McCauley MD, Strathdee SA, Benson CA, Pope RK, Leroux BM, Picel AC, Mateczun AJ, Cilwa KE, Regeimbal JM, Estrella LA, Wolfe DM, Henry MS, Quinones J, Salka S, Bishop-Lilly KA, Young R, Hamilton T. 2017. Development and use of personalized bacteriophage-based therapeutic cocktails to treat a patient with a disseminated resistant *Acinetobacter baumannii* infection. Antimicrob Agents Chemother 61.
8. Chan BK, Turner PE, Kim S, Mojibian HR, Elefteriades JA, Narayan D. 2018. Phage treatment of an aortic graft infected with Pseudomonas aeruginosa. Evol Med Public Health 2018:60-66.
9. Chatterjee A, Johnson CN, Luong P, Hullahalli K, McBride SW, Schubert AM, Palmer KL, Carlson PE, Jr., Duerkop BA. 2019. Bacteriophage resistance alters antibiotic-mediated intestinal expansion of enterococci. Infect Immun 87.
10. Chatterjee A, Willett JLE, Nguyen UT, Monogue B, Palmer KL, Dunny GM, Duerkop BA. 2020. Parallel genomics uncover novel enterococcal-bacteriophage interactions. mBio 11.
11. Duerkop BA, Huo W, Bhardwaj P, Palmer KL, Hooper LV. 2016. Molecular basis for lytic bacteriophage resistance in enterococci. mBio 7.
12. Wandro S, Oliver A, Gallagher T, Weihe C, England W, Martiny JBH, Whiteson K. 2018. Predictable molecular adaptation of coevolving *Enterococcus faecium* and lytic phage EfV12-phi1. Front Microbiol 9:3192.
13. Lossouarn J, Briet A, Moncaut E, Furlan S, Bouteau A, Son O, Leroy M, DuBow MS, Lecointe F, Serror P, Petit MA. 2019. *Enterococcus faecalis* countermeasures defeat a virulent Picovirinae bacteriophage. Viruses 11.
14. Ho K, Huo W, Pas S, Dao R, Palmer KL. 2018. Loss-of-function mutations in *epaR* confer resistance to phiNPV1 Infection in *Enterococcus faecalis* OG1RF. Antimicrob Agents Chemother 62.
15. Duerkop BA, Palmer KL, Horsburgh MJ. 2014. Enterococcal bacteriophages and genome defense. *In* Gilmore MS, Clewell DB, Ike Y, Shankar N (ed), Enterococci: from commensals to leading causes of drug resistant infection. Massachusetts Eye and Ear Infirmary, Boston.
16. Bolocan AS, Upadrasta A, Bettio PHA, Clooney AG, Draper LA, Ross RP, Hill C. 2019. Evaluation of phage therapy in the context of *Enterococcus faecalis* and its associated diseases. Viruses 11.
17. Palmer KL, Godfrey P, Griggs A, Kos VN, Zucker J, Desjardins C, Cerqueira G, Gevers D, Walker S, Wortman J, Feldgarden M, Haas B, Birren B, Gilmore MS. 2012. Comparative genomics of enterococci: variation in *Enterococcus faecalis*, clade structure in *E. faecium*, and defining characteristics of *E. gallinarum* and *E. casseliflavus*. mBio 3:e00318-11.
18. Ackermann HW. 2007. 5500 Phages examined in the electron microscope. Arch Virol 152:227-43.
19. Li L, Stoeckert CJ, Jr., Roos DS. 2003. OrthoMCL: identification of ortholog groups for eukaryotic genomes. Genome Res 13:2178-89.
20. Kim B, Wang YC, Hespen CW, Espinosa J, Salje J, Rangan KJ, Oren DA, Kang JY, Pedicord VA, Hang HC. 2019. *Enterococcus faecium* secreted antigen A generates muropeptides to enhance host immunity and limit bacterial pathogenesis. Elife 8.

21. Ittisoponpisan S, Islam SA, Khanna T, Alhuzimi E, David A, Sternberg MJE. 2019. Can predicted protein 3D structures provide reliable insights into whether missense variants are disease associated? J Mol Biol 431:2197-2212.
22. Rangan KJ, Pedicord VA, Wang YC, Kim B, Lu Y, Shaham S, Mucida D, Hang HC. 2016. A secreted bacterial peptidoglycan hydrolase enhances tolerance to enteric pathogens. Science 353:1434-1437.
23. Teng F, Kawalec M, Weinstock GM, Hryniewicz W, Murray BE. 2003. An *Enterococcus faecium* secreted antigen, SagA, exhibits broad-spectrum binding to extracellular matrix proteins and appears essential for *E. faecium* growth. Infect Immun 71:5033-41.
24. Djoric D, Kristich CJ. 2017. Extracellular SalB contributes to intrinsic cephalosporin resistance and cell envelope integrity in *Enterococcus faecalis*. J Bacteriol 199.
25. Guerardel Y, Sadovskaya I, Maes E, Furlan S, Chapot-Chartier MP, Mesnage S, Rigottier-Gois L, Serror P. 2020. Complete structure of the enterococcal polysaccharide antigen (EPA) of vancomycin-resistant *Enterococcus faecalis* V583 Reveals that EPA decorations are teichoic acids covalently linked to a rhamnopolysaccharide backbone. mBio 11.
26. Kortright KE, Chan BK, Koff JL, Turner PE. 2019. Phage therapy: a renewed approach to combat antibiotic-resistant bacteria. Cell Host Microbe 25:219-232.
27. Mangalea MR, Duerkop BA. 2020. Fitness trade-offs resulting from bacteriophage resistance potentiate synergistic antibacterial strategies. Infect Immun 88.
28. Morrisette T, Lev KL, Kebriaei R, Abdul-Mutakabbir J, Stamper KC, Morales S, Lehman SM, Canfield GS, Duerkop BA, Arias CA, Rybak MJ. 2020. Bacteriophage-antibiotic combinations for *Enterococcus faecium* with varying bacteriophage and daptomycin susceptibilities. Antimicrob Agents Chemother doi:10.1128/AAC.00993-20.
29. Rice LB, Lakticová V, Helfand MS, Hutton-Thomas R. 2004. In vitro antienterococcal activity explains associations between exposures to antimicrobial agents and risk of colonization by multiresistant enterococci. J Infect Dis 190:2162-6.
30. Ubeda C, Taur Y, Jenq RR, Equinda MJ, Son T, Samstein M, Viale A, Socci ND, van den Brink MR, Kamboj M, Pamer EG. 2010. Vancomycin-resistant *Enterococcus* domination of intestinal microbiota is enabled by antibiotic treatment in mice and precedes bloodstream invasion in humans. J Clin Invest 120:4332-41.
31. Brandl K, Plitas G, Mihu CN, Ubeda C, Jia T, Fleisher M, Schnabl B, DeMatteo RP, Pamer EG. 2008. Vancomycin-resistant enterococci exploit antibiotic-induced innate immune deficits. Nature 455:804-7.
32. Donskey CJ, Chowdhry TK, Hecker MT, Hoyen CK, Hanrahan JA, Hujer AM, Hutton-Thomas RA, Whalen CC, Bonomo RA, Rice LB. 2000. Effect of antibiotic therapy on the density of vancomycin-resistant enterococci in the stool of colonized patients. N Engl J Med 343:1925-32.
33. Hendrickx AP, Top J, Bayjanov JR, Kemperman H, Rogers MR, Paganelli FL, Bonten MJ, Willems RJ. 2015. Antibiotic-driven dysbiosis mediates intraluminal agglutination and alternative segregation of *Enterococcus faecium* from the intestinal epithelium. mBio 6:e01346-15.
34. Duan Y, Llorente C, Lang S, Brandl K, Chu H, Jiang L, White RC, Clarke TH, Nguyen K, Torralba M, Shao Y, Liu J, Hernandez-Morales A, Lessor L, Rahman IR, Miyamoto Y, Ly M, Gao B, Sun W, Kiesel R, Hutmacher F, Lee S, Ventura-Cots M, Bosques-Padilla F, Verna EC, Abraldes JG, Brown RS, Jr., Vargas V, Altamirano J, Caballeria J, Shawcross DL, Ho SB, Louvet A, Lucey MR, Mathurin P, Garcia-Tsao G, Bataller R, Tu XM, Eckmann L, van der Donk WA, Young R, Lawley TD, Starkel P, Pride D, Fouts DE,

Schnabl B. 2019. Bacteriophage targeting of gut bacterium attenuates alcoholic liver disease. Nature 575:505-511.

35. Stein-Thoeringer CK, Nichols KB, Lazrak A, Docampo MD, Slingerland AE, Slingerland JB, Clurman AG, Armijo G, Gomes ALC, Shono Y, Staffas A, Burgos da Silva M, Devlin SM, Markey KA, Bajic D, Pinedo R, Tsakmaklis A, Littmann ER, Pastore A, Taur Y, Monette S, Arcila ME, Pickard AJ, Maloy M, Wright RJ, Amoretti LA, Fontana E, Pham D, Jamal MA, Weber D, Sung AD, Hashimoto D, Scheid C, Xavier JB, Messina JA, Romero K, Lew M, Bush A, Bohannon L, Hayasaka K, Hasegawa Y, Vehreschild M, Cross JR, Ponce DM, Perales MA, Giralt SA, Jenq RR, Teshima T, Holler E, Chao NJ, et al. 2019. Lactose drives *Enterococcus* expansion to promote graft-versus-host disease. Science 366:1143-1149.

36. Baddour LM, Wilson WR, Bayer AS, Fowler VG, Jr., Tleyjeh IM, Rybak MJ, Barsic B, Lockhart PB, Gewitz MH, Levison ME, Bolger AF, Steckelberg JM, Baltimore RS, Fink AM, O'Gara P, Taubert KA, American Heart Association Committee on Rheumatic Fever E, Kawasaki Disease of the Council on Cardiovascular Disease in the Young CoCCCoCS, Anesthesia, Stroke C. 2015. Infective endocarditis in adults: diagnosis, antimicrobial therapy, and management of complications: a scientific statement for healthcare professionals from the American Heart Association. Circulation 132:1435-86.

37. Lorenzo MP, Kidd JM, Jenkins SG, Nicolau DP, Housman ST. 2019. In vitro activity of ampicillin and ceftriaxone against ampicillin-susceptible *Enterococcus faecium*. J Antimicrob Chemother 74:2269-2273.

38. Djoric D, Little JL, Kristich CJ. 2020. Multiple low-reactivity class B penicillin-binding proteins are required for cephalosporin resistance in enterococci. Antimicrob Agents Chemother 64.

39. Arbeloa A, Segal H, Hugonnet JE, Josseaume N, Dubost L, Brouard JP, Gutmann L, Mengin-Lecreulx D, Arthur M. 2004. Role of class A penicillin-binding proteins in PBP5-mediated beta-lactam resistance in Enterococcus faecalis. J Bacteriol 186:1221-8.

40. Rice LB, Carias LL, Rudin S, Hutton R, Marshall S, Hassan M, Josseaume N, Dubost L, Marie A, Arthur M. 2009. Role of class A penicillin-binding proteins in the expression of beta-lactam resistance in *Enterococcus faecium*. J Bacteriol 191:3649-56.

41. Sifaoui F, Arthur M, Rice L, Gutmann L. 2001. Role of penicillin-binding protein 5 in expression of ampicillin resistance and peptidoglycan structure in *Enterococcus faecium*. Antimicrob Agents Chemother 45:2594-7.

42. Triboulet S, Dubee V, Lecoq L, Bougault C, Mainardi JL, Rice LB, Etheve-Quelquejeu M, Gutmann L, Marie A, Dubost L, Hugonnet JE, Simorre JP, Arthur M. 2013. Kinetic features of L,D-transpeptidase inactivation critical for beta-lactam antibacterial activity. PLoS One 8:e67831.

43. Mainardi JL, Hugonnet JE, Rusconi F, Fourgeaud M, Dubost L, Moumi AN, Delfosse V, Mayer C, Gutmann L, Rice LB, Arthur M. 2007. Unexpected inhibition of peptidoglycan LD-transpeptidase from *Enterococcus faecium* by the beta-lactam imipenem. J Biol Chem 282:30414-22.

44. Singh KV, Murray BE. 2019. Loss of a major enterococcal polysaccharide antigen (Epa) by *Enterococcus faecalis* is associated with increased resistance to ceftriaxone and carbapenems. Antimicrob Agents Chemother 63.

45. Dale JL, Cagnazzo J, Phan CQ, Barnes AM, Dunny GM. 2015. Multiple roles for *Enterococcus faecalis* glycosyltransferases in biofilm-associated antibiotic resistance, cell envelope integrity, and conjugative transfer. Antimicrob Agents Chemother 59:4094-105.

46. Gaupp R, Lei S, Reed JM, Peisker H, Boyle-Vavra S, Bayer AS, Bischoff M, Herrmann M, Daum RS, Powers R, Somerville GA. 2015. *Staphylococcus aureus* metabolic adaptations during the transition from a daptomycin susceptibility phenotype to a daptomycin nonsusceptibility phenotype. Antimicrob Agents Chemother 59:4226-38.
47. Mechler L, Bonetti EJ, Reichert S, Flotenmeyer M, Schrenzel J, Bertram R, Francois P, Gotz F. 2016. Daptomycin tolerance in the *Staphylococcus aureus pitA6* mutant is due to upregulation of the *dlt* operon. Antimicrob Agents Chemother 60:2684-91.
48. Bertsche U, Weidenmaier C, Kuehner D, Yang SJ, Baur S, Wanner S, Francois P, Schrenzel J, Yeaman MR, Bayer AS. 2011. Correlation of daptomycin resistance in a clinical *Staphylococcus aureus* strain with increased cell wall teichoic acid production and D-alanylation. Antimicrob Agents Chemother 55:3922-8.
49. Mello SS, Van Tyne D, Lebreton F, Silva SQ, Nogueira MCL, Gilmore MS, Camargo I. 2020. A mutation in the glycosyltransferase gene *lafB* causes daptomycin hypersusceptibility in *Enterococcus faecium*. J Antimicrob Chemother 75:36-45.
50. Sieradzki K, Tomasz A. 1997. Inhibition of cell wall turnover and autolysis by vancomycin in a highly vancomycin-resistant mutant of *Staphylococcus aureus*. Journal of Bacteriology 179:2557-2566.
51. Xu Y, Singh KV, Qin X, Murray BE, Weinstock GM. 2000. Analysis of a gene cluster of *Enterococcus faecalis* involved in polysaccharide biosynthesis. Infect Immun 68:815-23.
52. Rigottier-Gois L, Madec C, Navickas A, Matos RC, Akary-Lepage E, Mistou MY, Serror P. 2015. The surface rhamnopolysaccharide epa of *Enterococcus faecalis* is a key determinant of intestinal colonization. J Infect Dis 211:62-71.
53. Mohamed JA, Huang W, Nallapareddy SR, Teng F, Murray BE. 2004. Influence of origin of isolates, especially endocarditis isolates, and various genes on biofilm formation by *Enterococcus faecalis*. Infect Immun 72:3658-63.
54. Ramos Y, Rocha J, Hael AL, van Gestel J, Vlamakis H, Cywes-Bentley C, Cubillos-Ruiz JR, Pier GB, Gilmore MS, Kolter R, Morales DK. 2019. PolyGlcNAc-containing exopolymers enable surface penetration by non-motile *Enterococcus faecalis*. PLoS Pathog 15:e1007571.
55. Breton YL, Mazé A, Hartke A, Lemarinier S, Auffray Y, Rincé A. 2002. Isolation and characterization of bile salts-sensitive mutants of *Enterococcus faecalis*. Current Microbiology 45:0434-0439.
56. Rincé A, Le Breton Y, Verneuil N, Giard J-C, Hartke A, Auffray Y. 2003. Physiological and molecular aspects of bile salt response in *Enterococcus faecalis*. International Journal of Food Microbiology 88:207-213.
57. Mohamed JA, Teng F, Nallapareddy SR, Murray BE. 2006. Pleiotrophic effects of 2 *Enterococcus faecalis sagA*-like genes, *salA* and *salB*, which encode proteins that are antigenic during human infection, on biofilm formation and binding to collagen type i and fibronectin. J Infect Dis 193:231-40.
58. Shankar J, Walker RG, Wilkinson MC, Ward D, Horsburgh MJ. 2012. SalB inactivation modulates culture supernatant exoproteins and affects autolysis and viability in *Enterococcus faecalis* OG1RF. J Bacteriol 194:3569-78.
59. Aziz RK, Bartels D, Best AA, DeJongh M, Disz T, Edwards RA, Formsma K, Gerdes S, Glass EM, Kubal M, Meyer F, Olsen GJ, Olson R, Osterman AL, Overbeek RA, McNeil LK, Paarmann D, Paczian T, Parrello B, Pusch GD, Reich C, Stevens R, Vassieva O, Vonstein V, Wilke A, Zagnitko O. 2008. The RAST Server: rapid annotations using subsystems technology. BMC Genomics 9:75.
60. Mijalis E, Rasche H. 2013-2017. CPT galaxy tools. https://github.com/tamu-cpt/galaxy-tools/ Accessed 1 May 2020.

61. Hyatt D, Chen GL, Locascio PF, Land ML, Larimer FW, Hauser LJ. 2010. Prodigal: prokaryotic gene recognition and translation initiation site identification. BMC Bioinformatics 11:119.
62. Nishimura Y, Yoshida T, Kuronishi M, Uehara H, Ogata H, Goto S. 2017. ViPTree: the viral proteomic tree server. Bioinformatics 33:2379-2380.
63. Perez-Casal J, Caparon MG, Scott JR. 1991. Mry, a trans-acting positive regulator of the M protein gene of *Streptococcus pyogenes* with similarity to the receptor proteins of two-component regulatory systems. J Bacteriol 173:2617-24.
64. Shepard BD, Gilmore MS. 1995. Electroporation and efficient transformation of *Enterococcus faecalis* grown in high concentrations of glycine. Methods Mol Biol 47:217-26.
65. Zhang X, Paganelli FL, Bierschenk D, Kuipers A, Bonten MJ, Willems RJ, van Schaik W. 2012. Genome-wide identification of ampicillin resistance determinants in *Enterococcus faecium*. PLoS Genet 8:e1002804.
66. Mihara T, Nishimura Y, Shimizu Y, Nishiyama H, Yoshikawa G, Uehara H, Hingamp P, Goto S, Ogata H. 2016. Linking virus genomes with host taxonomy. Viruses 8:66.

Figure Legends.

Figure 1. Genome organization and morphogenesis of three previously uncharacterized *E. faecium* phages. Whole genome sequencing reveals a modular functional organization of phage 9181, 9183 and 9184 genomes. Open reading frames for each phage were determined by RAST version 2.0 and by the Texas A&M Center for Phage Therapy structural analysis workflow version 2020.01. Colored open reading frames correspond to the functional prediction. Beneath the phage genome maps, TEM shows phage 9181, 9183 and 9184 are non-contractile tailed *Siphoviridae*. The *E. faecium* host strain for phage 9181 is *E. faecium* Com12. The host strain for phage 9183 and 9184 is *E. faecium* 1,141,733.

Figure 2. Comparative genomic analysis identifies two novel enterococcal phage orthoclusters. A comparative genome analysis was performed using OrthoMCL as described previously by Bolocan et al. (16). A phylogenetic proteomic tree was constructed from the OrthoMCL matrix using the Manhattan distance metric and hierarchical clustering using an average linkage with 1000 iterations. Ninety-nine enterococcal phage genomes available from NCBI were used for comparison to *E. faecium* phages 9181, 9183, and 9184 (highlighted in red). Distinct phage orthoclusters are represented by colored boxes. Roman numerals to the right of the shaded boxes signify the phage orthocluster number. Phage

854 orthocluster morphology is indicated by calipers (if known) or an asterisk symbol (if unknown) to the
855 right of the roman numerals.
856
857 **Figure 3. *E. faecium* phages demonstrate broad and narrow host ranges.** Host ranges of phage
858 9181, 9183, and 9184. Phage 9181 and 9183 have a narrow *E. faecium* host range, while phage 9184
859 shows a broader host range. Bacteria were susceptible if less than 1 x 10^5 CFU/mL of bacteria were
860 recovered from a phage susceptibility assay. Bacteria were resistant if greater than 1 x 10^5 CFU/mL of
861 bacteria were recovered from a phage susceptibility assay. (A) Indicates host range for a collection of
862 laboratory strains. (B) Indicates the host range for a collection of clinical isolates provided by the clinical
863 microbiology lab at the University of Colorado, Anschutz Medical Campus.
864
865 **Figure 4. *E. faecium* elicits a robust resistance phenotype to phage 9181 and 9183, but variable**
866 **resistance to phage 9184.** Representative phage resistant strains raised against phages 9181 (A),
867 9183 (B), and 9184 (C). Data show phage susceptibility assays and associated bacterial enumeration
868 of wild type and phage resistant mutants in the presence (white bars) or absence (black bars) of phage
869 from three independent experiments. Error bars indicate standard deviation. Phage 9181 resistant (A)
870 and phage 9183 resistant (B) strains exhibit ≥ 4-log of survival in the presence of phages compared to
871 the parental *E. faecium* Com12 and 1,141,733 (733) strains, respectively. Phage 9184 resistant strains
872 (C) exhibit diverse resistance strength characterized weak (84R2) and strong (84R6) resistance
873 phenotypes. The dotted line indicates the spontaneous mutation threshold conferring phage resistance
874 observed in the respective wild type host strain of each phage.
875
876 **Figure 5. A diverse assortment of mutations confer phage resistance in *E. faecium*.** (A) Protein
877 secondary structure of *E. faecium* Com12 SagA, consisting of an N-terminus coiled-coil domain
878 (residues 18-242) and C-terminus NlpC_P60 peptidoglycan hydrolase domain (residues 393-520).
879 Displayed above the protein structure are colored lollipops denoting the site of mutations within
880 NlpC_P60 domain of phage 9181-resistant mutants. Inside and below the protein structure are colored

one letter amino acid abbreviations and lines, respectively, corresponding to key active site (red) and peptidoglycan clamp residues (teal) of the NlpC_P60 domain. Abbreviations: W, tryptophan; C, Cysteine; H, Histidine; G, Glycine; D, Aspartate; L, Leucine; Y, Tyrosine; V, Valine. (B) Capsule locus mutations are detected in a tyrosine kinase (*wze*), aminotransferase (*efsg_rs08090*), *wzy* (*efsg_rs08105*), and nucleotide sugar dehydrogenase (*efsg_rs08120*) of phage 9184-resistant mutants. Arrows indicate open reading frames. Arrow colors correspond to colored boxes (figure bottom left) indicate predicted open reading frame function (17). Colored lollipops above the arrows corresponding to colored dots (figure bottom right) indicate the mutational type. *E. faecium* 1,141,733 locus tags are angled below the arrows. (C) A missense mutation is found within a predicted arginine-aspartate-aspartate protein (*rdd*; black arrow) of one phage 9184-resistant mutant (84R6) of *E. faecium* 1,141,733. *rdd* is flanked upstream by a predicted hypothetical protein (white arrow) and signal sequence peptidase A (*sspA*; black arrow) and downstream by another hypothetical protein (white arrow). *E. faecium* 1,141,733 locus tags are angled below the arrows. (D) Mutations in predicted teichoic acid biosynthesis genes (*epaR* and *epaX*) are identified in phage 9183-resistant mutants of *E. faecium* 1,141,733 (25). Arrow colors correspond to colored boxes (figure bottom left) indicate predicted open reading frame function. Colored lollipops above the arrows corresponding to colored dots (figure bottom right) indicate the mutational type. *E. faecium* 1,141,733 locus tags are angled below the arrows. The brackets above the locus correspond the conserved (left) and variable (right) portions of the *epa* locus proposed to by Gueredal et al. to encode the machinery necessary for rhamnopolysaccharide synthesis and wall teichoic acid biosynthesis, respectively (25).

Figure 6. Mutation in the capsule and exopolysaccharide loci limit phage adsorption in *E. faecium*. Shown is the fold-change in phage 9181 (A), 9183 (B), and 9184 (C) adsorption compared to wild type (WT) *E. faecium*. Results represent average fold-change and standard deviation from three independent experiments. *, $P < 0.05$; **, $P < 0.01$ using an unpaired Student's *t* test.

907 **Figure 7. Phage 9181 and phage 9183 synergize with antibiotics to kill *E. faecium*.** (A-E) *E.*
908 *faecium* growth was monitored over 18 hours in the presence of phage (open blue squares), sub-
909 inhibitory concentrations of antibiotics (open orange, grey, purple triangles or diamonds), both phage
910 and sub-inhibitory concentration of antibiotics (filled orange, grey and purple triangles or diamonds), or
911 media alone (open black circles). Phage 9181 was used in experiments with *E. faecium* Com12, while
912 phage 9183 was employed for experiments with 1,141,733. Phages 9181 (A) and 9183 (B) synergize
913 with sub-inhibitory concentration of ampicillin (AMP) in a dose responsive manner to kill *E. faecium*
914 Com12 and 1,141,733, respectively. Phage 9181 (C) and 9183 (D) synergize with sub-inhibitory
915 concentrations of ceftriaxone (CTX) to kill *E. faecium* Com12 and 1,141,733, respectively. Phage 9183
916 (E) synergizes with sub-inhibitory concentrations of daptomycin (DAP) in a dose-responsive manner to
917 kill *E. faecium* 1,141,733. Three technical replicates were performed for each condition tested and the
918 averages plotted. Error bars indicate standard deviation. Shown are the results from one experiment
919 that was replicated in triplicate.
920
921 **Supplemental Figure Legends**
922 **Figure S1. *Enterococcus faecium* phage orthoclusters.** Phage protein coding sequence alignments
923 were performed with nearest neighbors in VIP Tree (62, 66). Colored lines connecting genomes
924 indicate percent protein identity along the length of each genome. (A) Phage 9183 demonstrates
925 protein homology and similar genome organization to its nearest neighbor intra-orthocluster phages
926 (phages VFW and VPE25). (B) Phage 9184 demonstrates proteome homology and similar genome
927 organization to its nearest neighbor intra-orthocluster phages (phages vB EfaS-DELF1 and IME-EFm5).
928 (C) Phage 9181 shows little to no protein homology to its nearest neighbor extra-orthocluster phages
929 (phages EFC-1 and FLA4).
930
931 **Figure S2. Phage resistant mutants of E. faecium following exposure to phages 9181, 9183 and**
932 **9184.** Phage 9181 (A), 9183 (B), and 9184 susceptibility assays and associated bacterial enumeration
933 of wild type and phage resistant mutants in the presence (white bars) or absence (black bars) of phage

(A-F) from three independent experiments. Phage 9181 (A, C) and phage 9183 (B, E) resistant strains exhibit ≥ 5-logs of survival versus *E. faecium* Com12 and 1,141,733 (i.e. 733), respectively. Phage 9184 resistant strains exhibit a weak resistance phenotypes. The dotted line indicates the spontaneous mutation threshold conferring phage resistance observed in the respective wild type host strain of each phage.

Figure S3. SagA is conserved in *E. faecium* Com12 and Com15. Displayed is the BLASTP alignment of SagA between Com12 and Com15, showing 95% similarity and strict conservation of peptidoglycan clamp (orange lettering) and active site residues (red lettering). Colored highlights indicate the location of amino acid changes detected in phage 9181 resistant mutants (81R3 and 81R4 – green highlight, 81R5 – yellow highlight, 81R6 – blue highlight, 81R8 – magenta highlight). Specific amino acid changes are noted below the alignment in parentheses next to their respective phage resistant mutant.

Figure S4. Complementation restores phage susceptibility in phage resistant mutants. Bacterial enumeration from Phage 9181 (A and B), 9184 (C), and 9183 (D) phage susceptibility assays of wild type and phage resistant mutants complemented with their respective wild type allele or empty vector. Assays were performed in the presence (white bars) or absence (black bars) of phages from two independent experiments. The bars and error bars indicate the average and standard deviation from two independent experiments. The dotted line indicates the spontaneous mutation threshold conferring phage resistance observed in the respective wild type host strain of each phage.

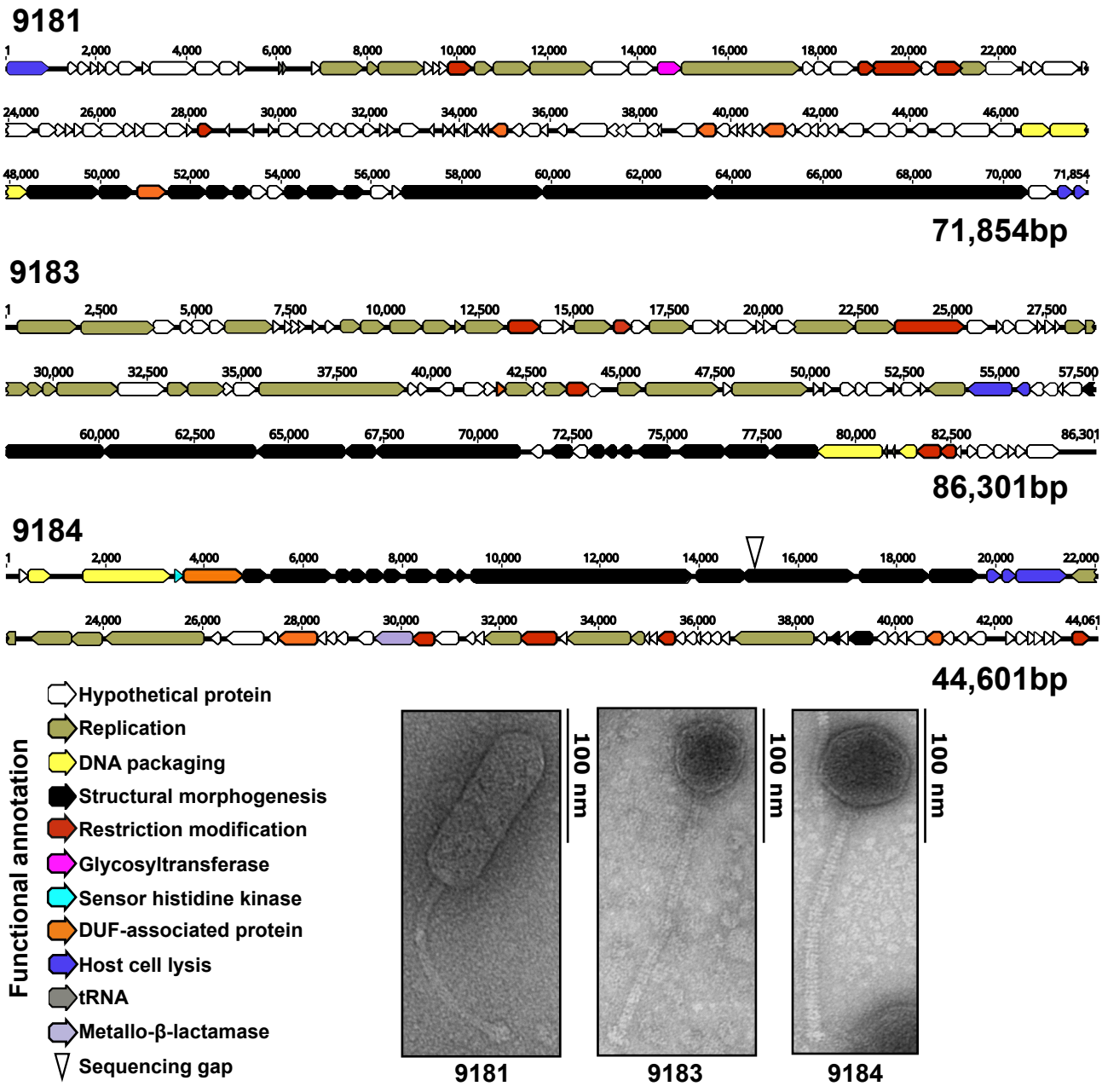

Figure 1

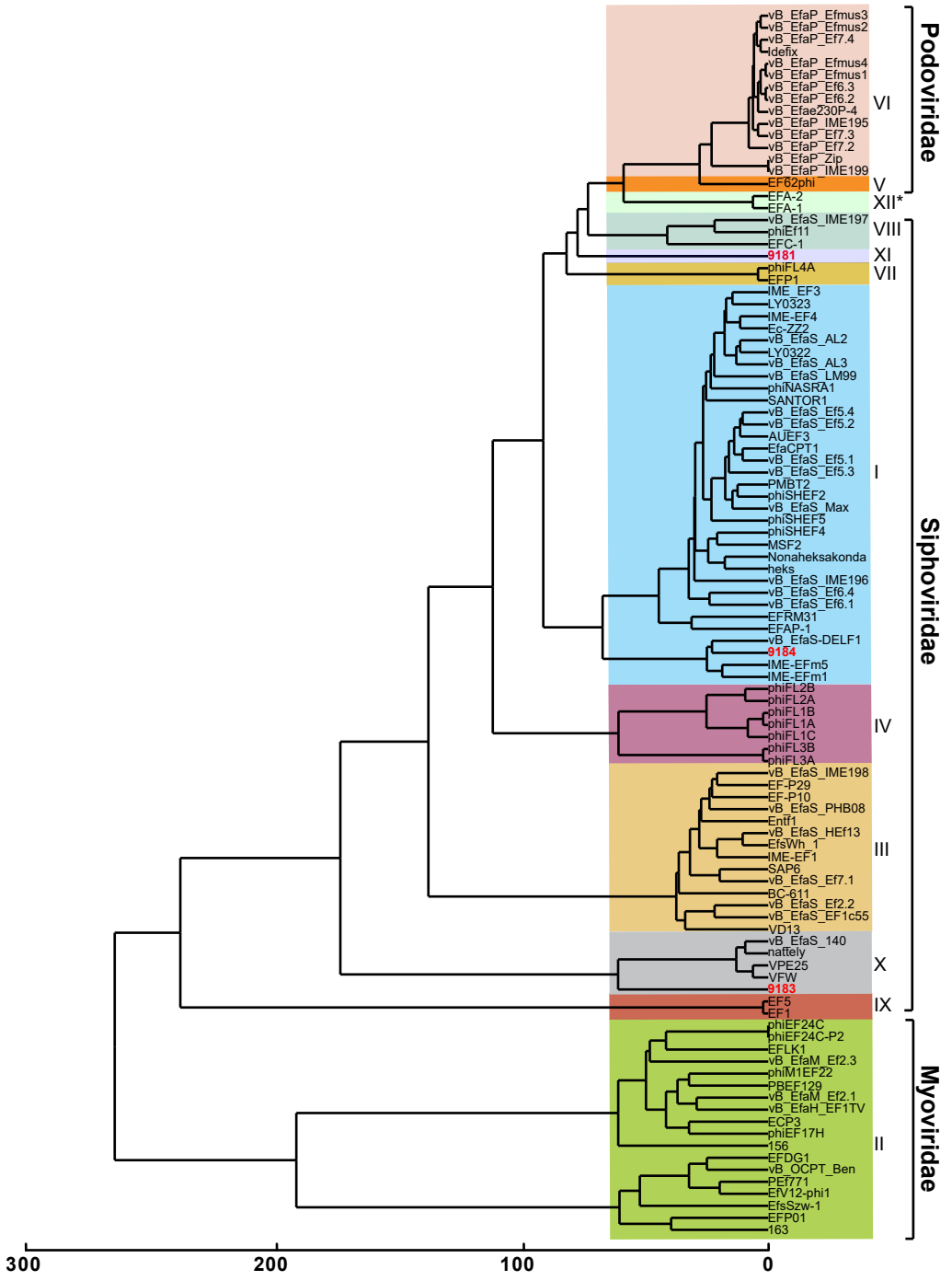

Figure 2

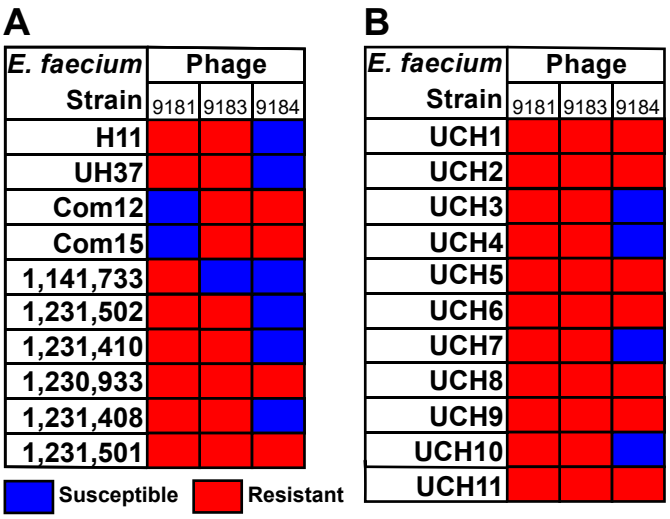

Figure 3

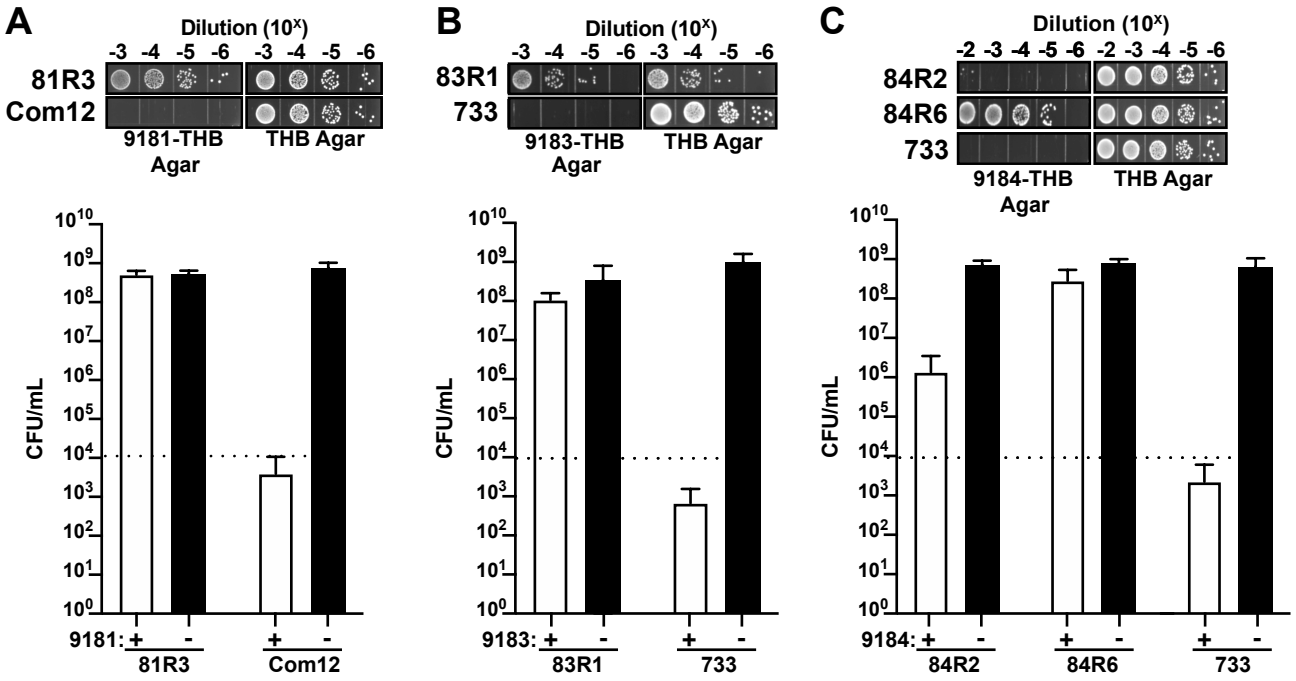

Figure 4

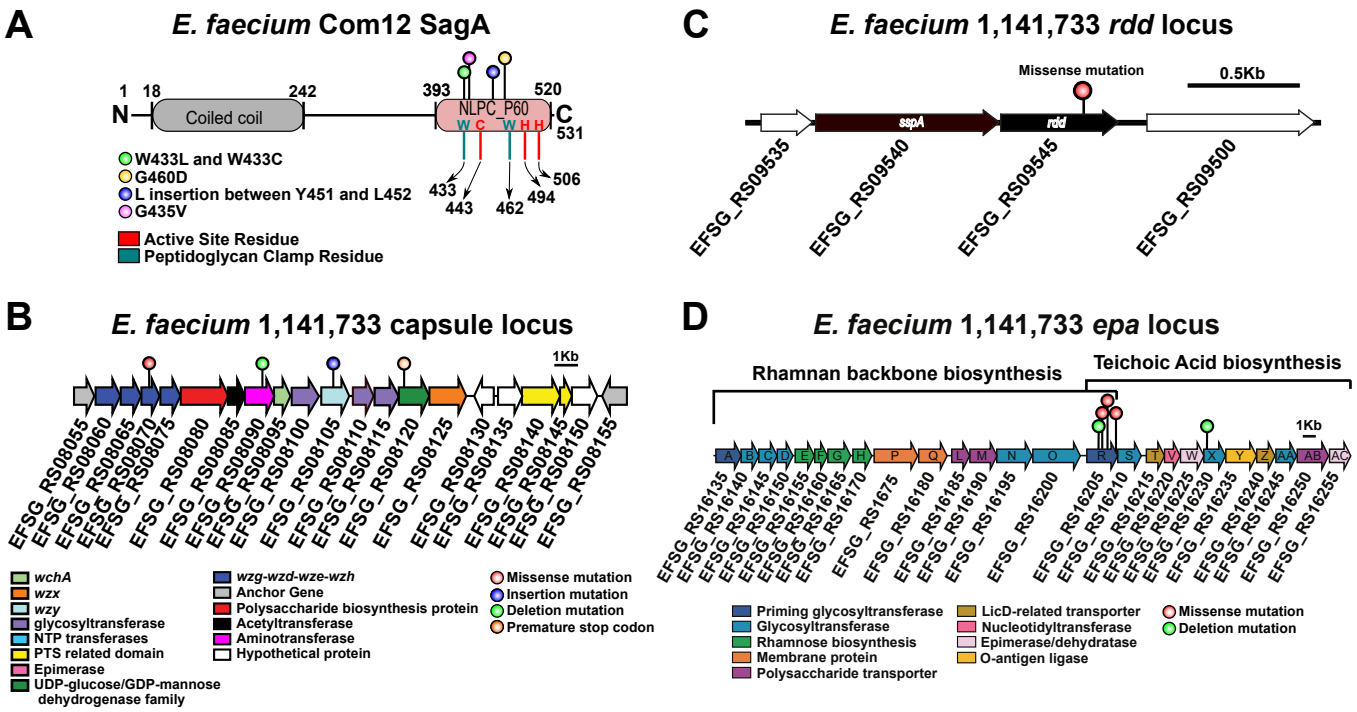

Figure 5

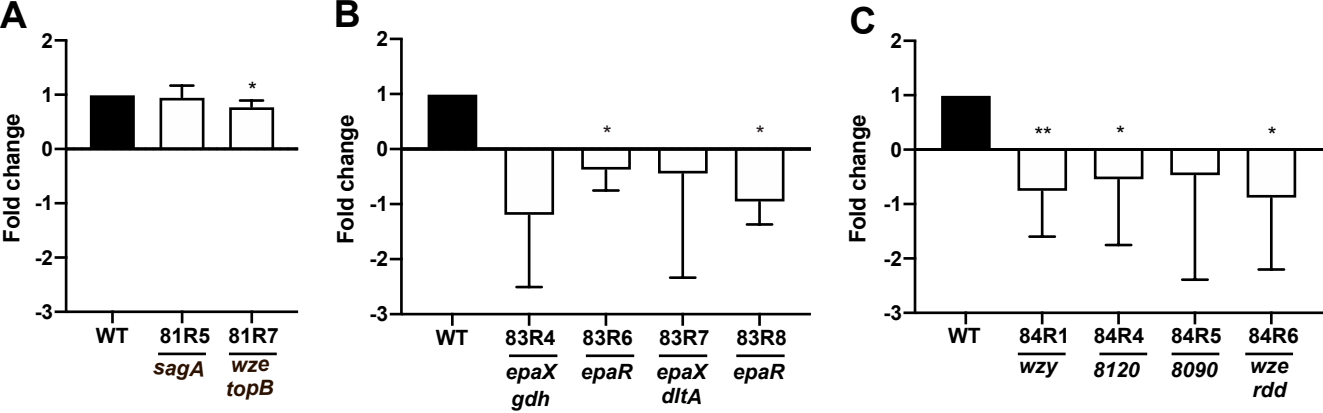
A
B
C
Fold change
2
1
0
-1
-2
-3
*
**
WT
81R5
sagA
81R7
wze
topB
83R4
epaX
gdh
83R6
epaR
83R7
epaX
dltA
83R8
epaR
84R1
wzy
84R4
8120
84R5
8090
84R6
wze
rdd

Figure 6

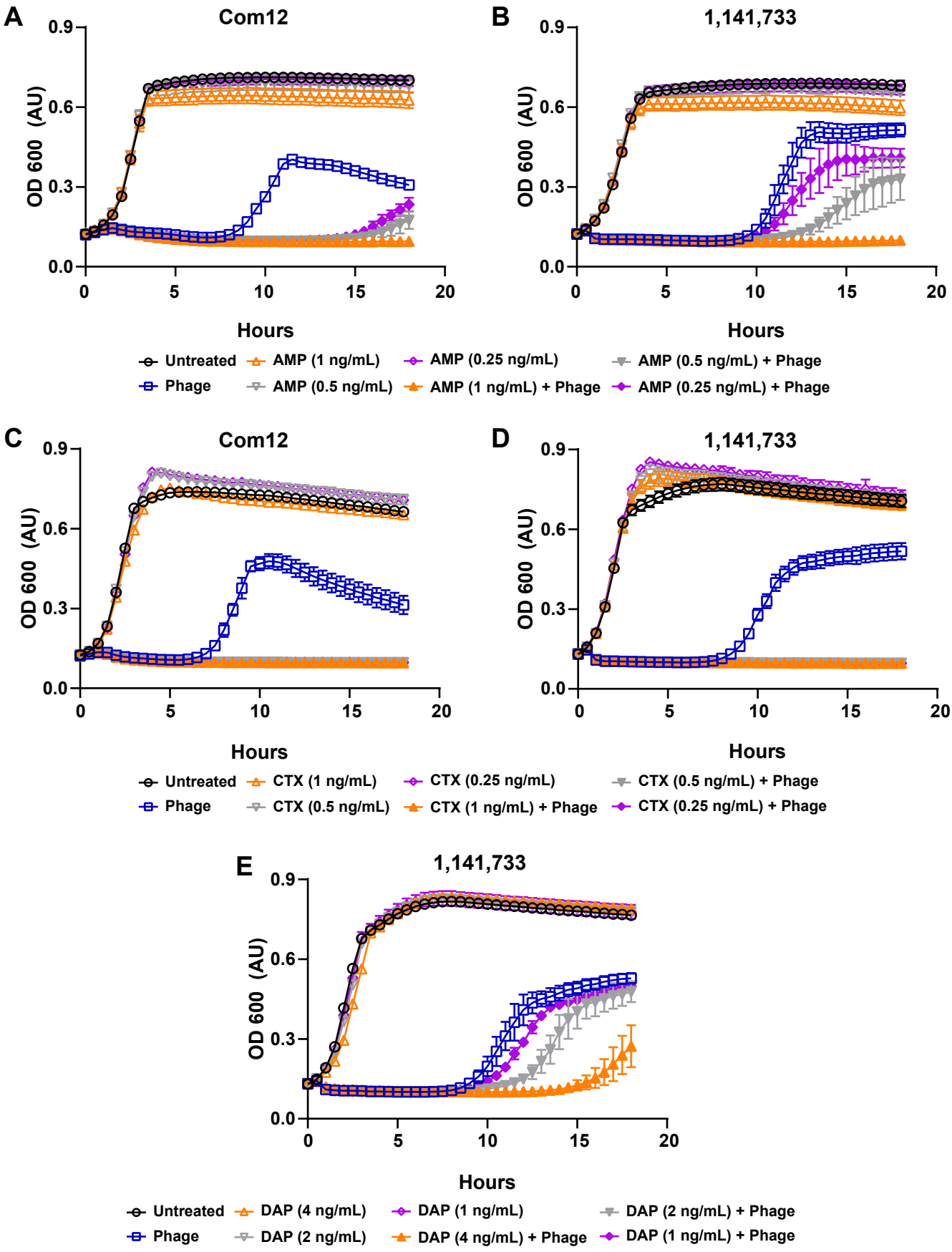

Figure 7

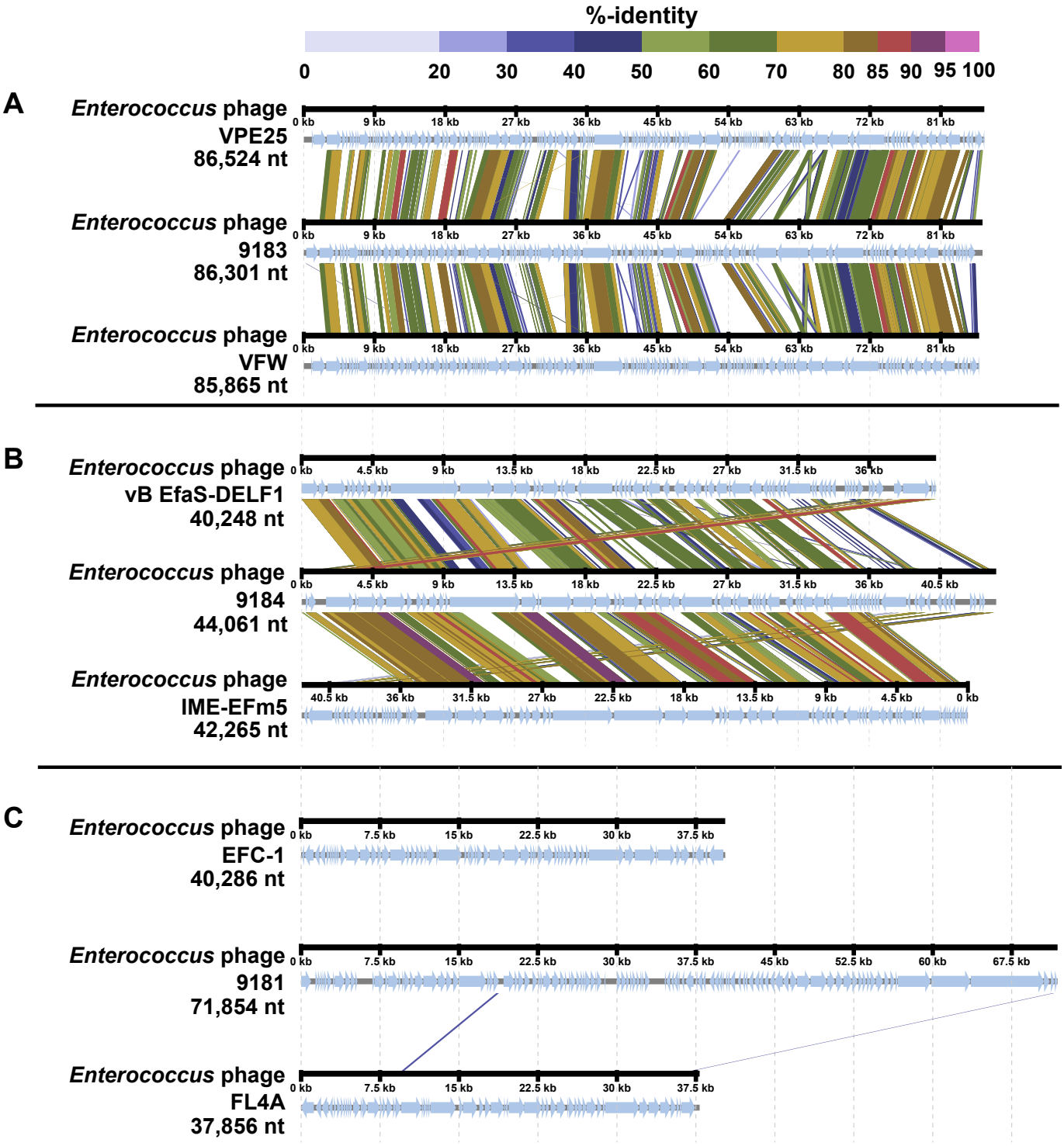

Figure S1

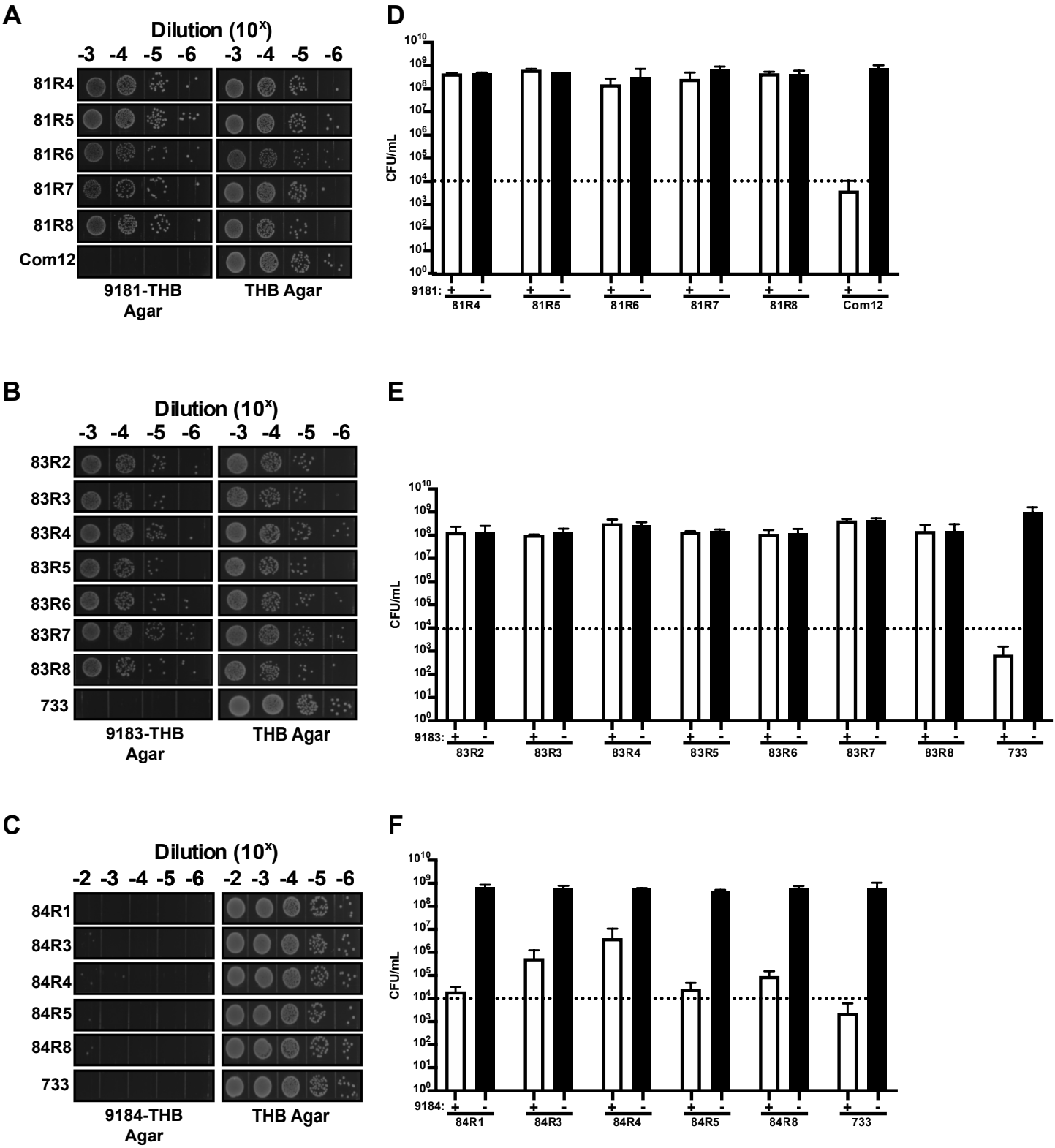

Figure S2

Identities	Positives	Gaps
513/538(95%)	515/538(95%)	20/538(3%)

```
Com12  1    VKKSLISAVMVCSMTLTAVASPIAAAADDFDSQIQQQDQKIADLKNQQADAQSQIDALES  60
           +KKSLISAVMVCSMTLTAVASPIAAAADDFDSQIQQQDQKIADLKNQQADAQSQIDALES
Com15  1    MKKSLISAVMVCSMTLTAVASPIAAAADDFDSQIQQQDQKIADLKNQQADAQSQIDALES  60

Com12  61   QVSEINTQAQDLLAKQDTLRQESAQLVKDIADLQERIEKREDTIQKQAREAQVSNTSSNY  120
           QVSEINTQAQDLLAKQDTLRQESAQLVKDIADLQERIEKREDTIQKQAREAQVSNTSSNY
Com15  61   QVSEINTQAQDLLAKQDTLRQESAQLVKDIADLQERIEKREDTIQKQAREAQVSNTSSNY  120

Com12  121  IDAVLNADSLADAIGRVQAMTTMVKANNDLMEQQKQDKKAVEDKKAENDAKLKELAENQA  180
           IDAVLNADSLADAIGRVQAMTTMVKANNDLMEQQKQDKKAVEDKKAENDAKLKELAENQA
Com15  121  IDAVLNADSLADAIGRVQAMTTMVKANNDLMEQQKQDKKAVEDKKAENDAKLKELAENQA  180

Com12  181  ALESQKGDLLSKQADLNVLKTSLAAEQATAEDKKADLNRQKAEAEAEQARIREQQRLAEQ  240
           ALESQKGDLLSKQADLNVLKTSLAAEQATAEDKKADLNRQKAEAEAEQARIREQQRLAEQ
Com15  181  ALESQKGDLLSKQADLNVLKTSLAAEQATAEDKKADLNRQKAEAEAEQARIREQQRLAEQ  240

Com12  241  ARQQAAQEKAEKEAREQAEAEAQATQASSTAQSSASEESSAAQSSTTEESSSAAQSSTTE  300
           ARQQAAQEKAEKEAREQAEAEAQATQASS AQSSA+EESSAAQSSTTEESSSAAQSSTTE
Com15  241  ARQQAAQEKAEKEAREQAEAEAQATQASSAAQSSATEESSAAQSSTTEESSSAAQSSTTE  300

Com12  301  ESTTAPESSTTEESTTAPESSTTEESTTVPESSTTEESTTVPESSTTEESTTVPESSTTE  360
           ESTTAPESSTTEESTT PESSTTEESTT PESSTTEESTTVPESSTTEESTTVPES
Com15  301  ESTTAPESSTTEESTTXPESSTTEESTTAPESSTTEESTTVPESSTTEESTTVPES----  356

Com12  361  ESTTVPETSTEESTTPAPTTPSTDQSVDPGNSTGSNATNNT--------TNTTPTPTPSG  412
                   STEESTTPAPTTPSTDQSVDPGNSTGSNATNNT        TNTTPTPTPSG
Com15  357  --------STEESTTPAPTTPSTDQSVDPGNSTGSNATNNTTNTTPXXXTNTTPTPTPSG  408

Com12  413  SVNGAAIVAEAYKYIGTPYVWGGKDPSGFDCSGFTRYVYLQVTGRDIGGWTVPQESAGTK  472
           SVNGAAIVAEAYKYIGTPYVWGGKDPSGFDCSGFTRYVYLQVTGRDIGGWTVPQESAGTK
Com15  409  SVNGAAIVAEAYKYIGTPYVWGGKDPSGFDCSGFTRYVYLQVTGRDIGGWTVPQESAGTK  468

Com12  473  ISVSQAKAGDLLFWGSPGGTYHVAIALGGGQYIHAPQPGESVKVGSVQWFAPDFAVSM  530
           ISVSQAKAGDLLFWGSPGGTYHVAIALGGGQYIHAPQPGESVKVGSVQWFAPDFAVSM
Com15  469  ISVSQAKAGDLLFWGSPGGTYHVAIALGGGQYIHAPQPGESVKVGSVQWFAPDFAVSM  526
```

81R3 and 81R4 (W433G and W433C, respectively)
81R5 (G460D)
81R6 (note: L insertion between Y451 and L452
81R8 (G435V)
Active Site Residues (C443, H494, H506)
Peptidoglycan Clamp Residues (W433 and W462)

Figure S3

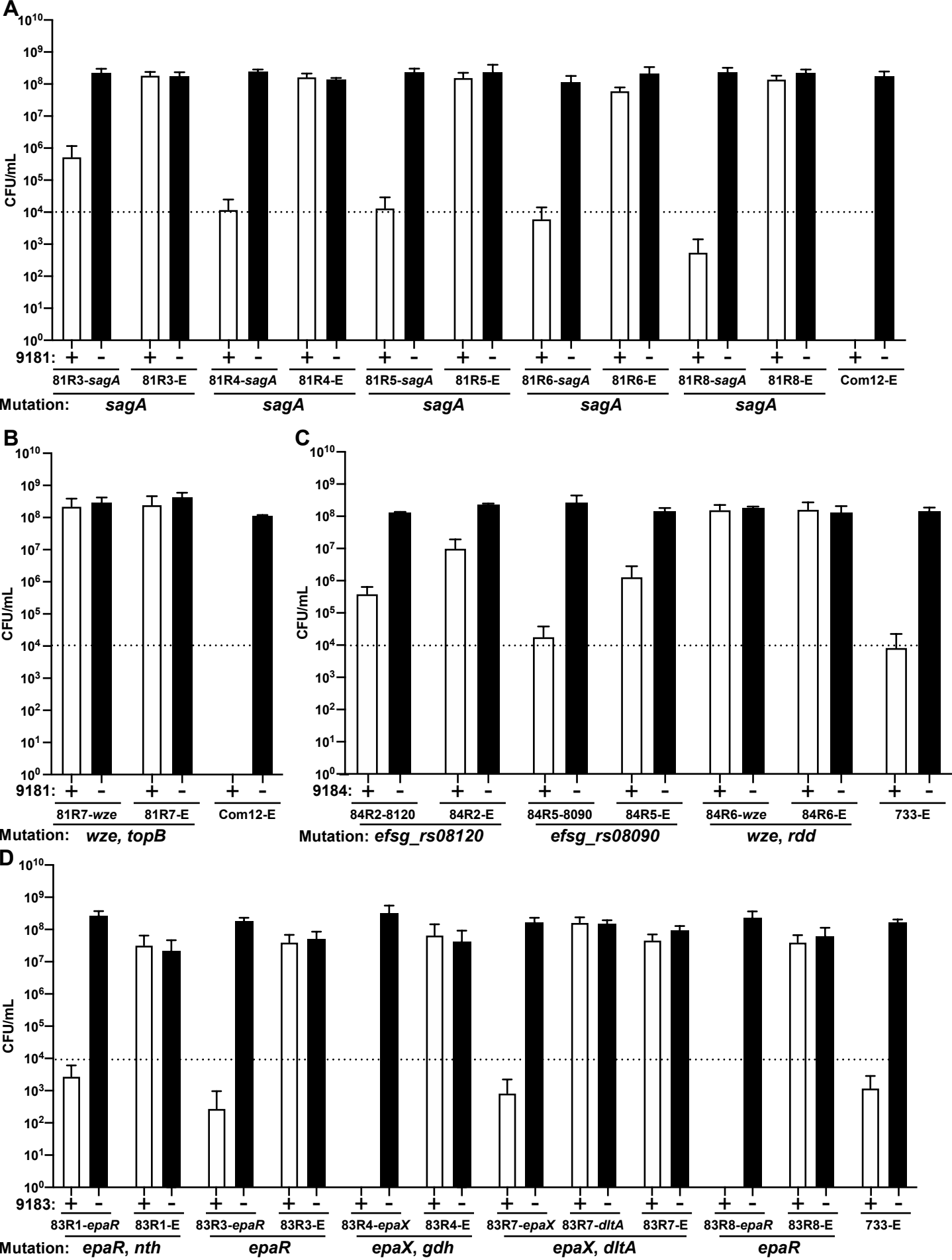
A
CFU/mL
9181:
81R3-sagA
81R3-E
81R4-sagA
81R4-E
81R5-sagA
81R5-E
81R6-sagA
81R6-E
81R8-sagA
81R8-E
Com12-E
Mutation: sagA
B
9181:
81R7-wze
81R7-E
Com12-E
Mutation: wze, topB
C
9184:
84R2-8120
84R2-E
84R5-8090
84R5-E
84R6-wze
84R6-E
733-E
Mutation: efsg_rs08120
efsg_rs08090
wze, rdd
D
9183:
83R1-epaR
83R1-E
83R3-epaR
83R3-E
83R4-epaX
83R4-E
83R7-epaX
83R7-dltA
83R7-E
83R8-epaR
83R8-E
733-E
Mutation: epaR, nth
epaR
epaX, gdh
epaX, dltA
epaR

Figure S4